

LHAASO observation of very high energy gamma-ray emission beyond 10 TeV from GRB 221009A

Xiao-Jun Bi (毕效军)

Institute of High Energy Physics, CAS

Vulcano workshop, Ischia (Naples, Italy)

May 26 - June 1, 2024

Outline

- Brief introduction of LHAASO
- LHAASO observation of GRB 221009A
- Implications of the observation
- Summary

LHAASO: Large High Altitude Air Shower Observatory

2008年4月开始R&D

2015年12月approved

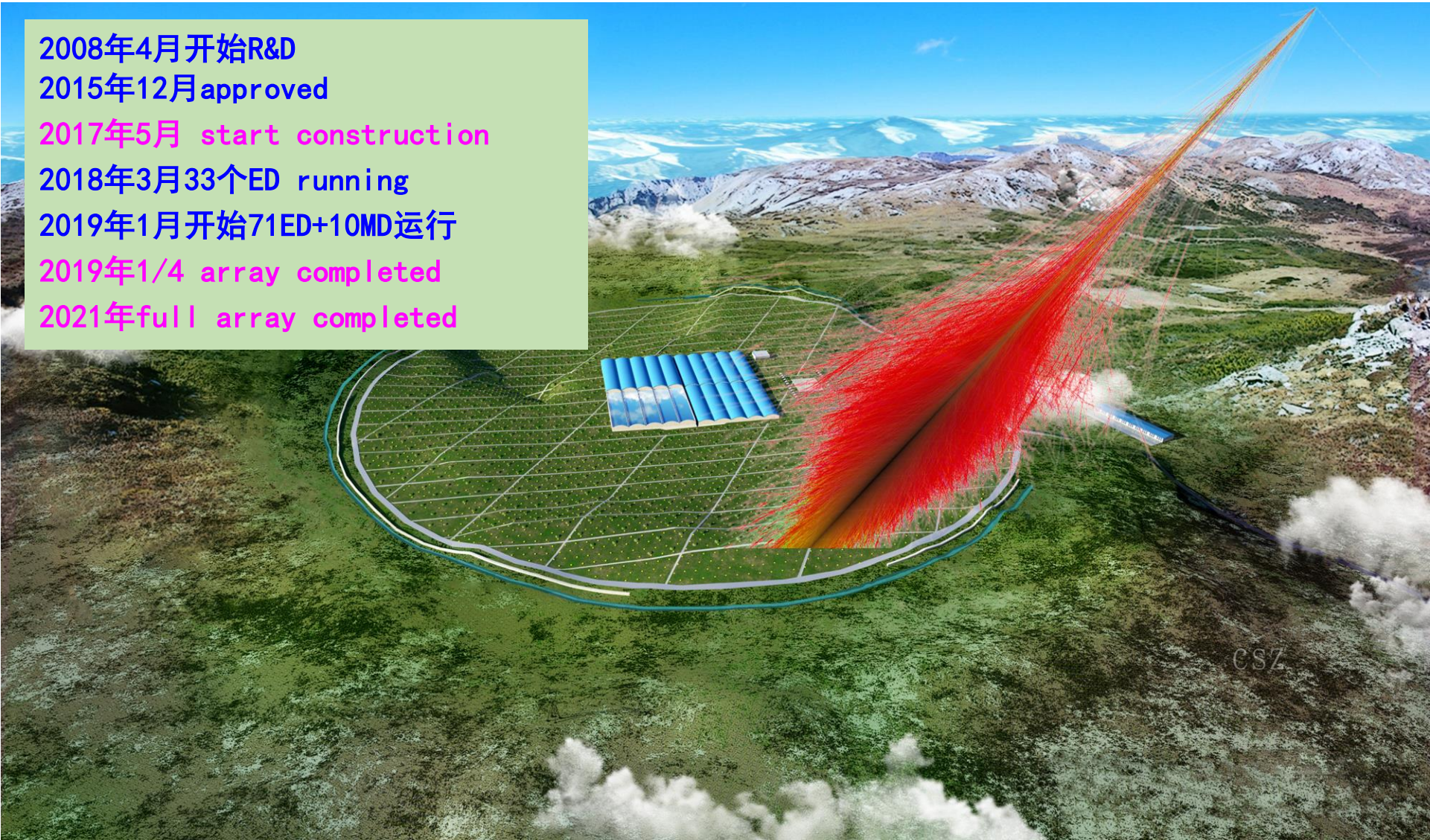
2017年5月 start construction

2018年3月33个ED running

2019年1月开始71ED+10MD运行

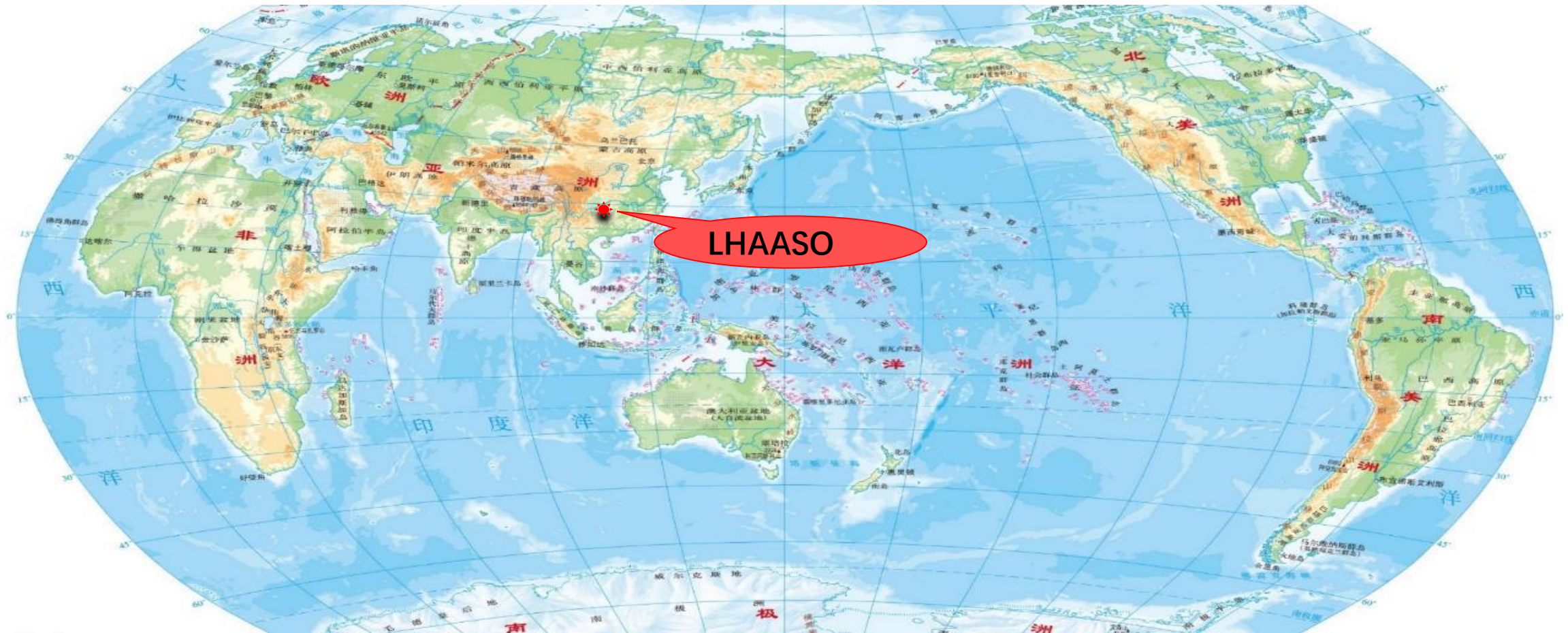
2019年1/4 array completed

2021年full array completed



Where is LHAASO?

- Haizi Mountain, Sichuan province, **China**
- Altitude **4410 m a.s.l.**
- Location: **29°21'27.6" N, 100°08'19.6" E.**



LHAASO aerial image, 2021/12

Area : 1.3km²



LHAASO detectors

KM2A

The best UHE
gamma-ray detector
4 TeV-20 TeV-10 PeV



WCDA

The best VHE gamma-
ray survey detector
0.1 TeV-20 TeV



WFCTA+KM2A+WCDA

The best cosmic ray
detector
10 TeV-100 PeV

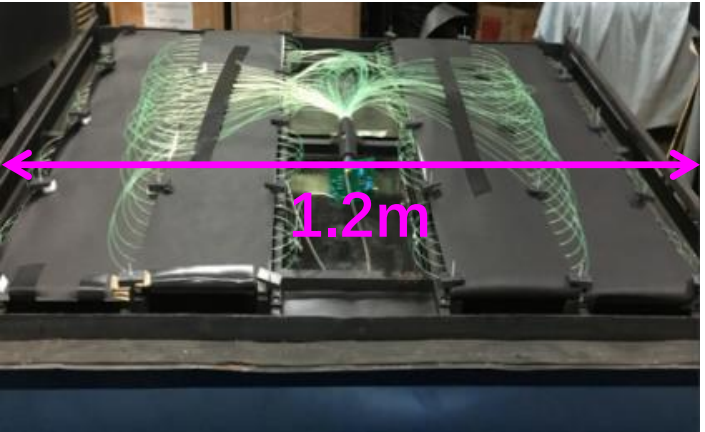


LHAASO detectors

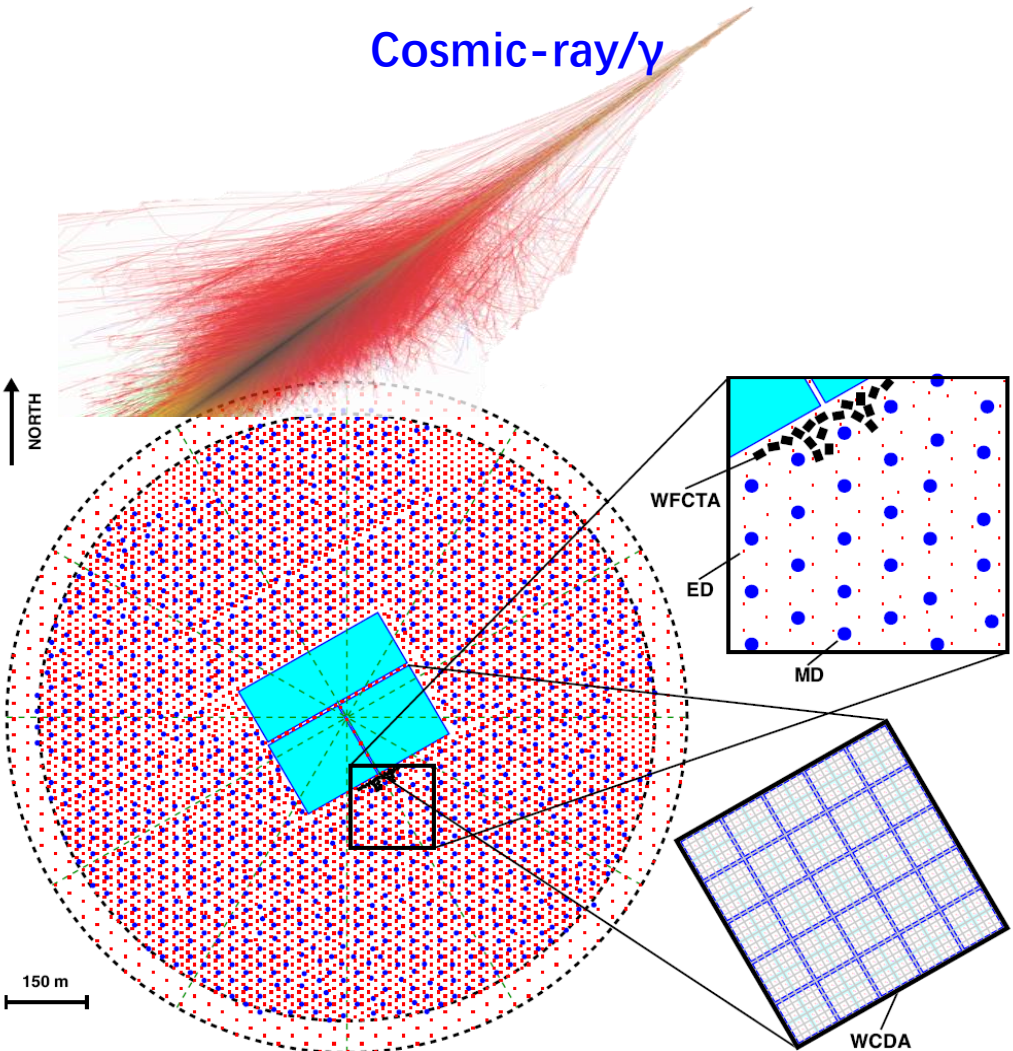
KM2A



MD: 1188x36m²



ED: 5216x1m²

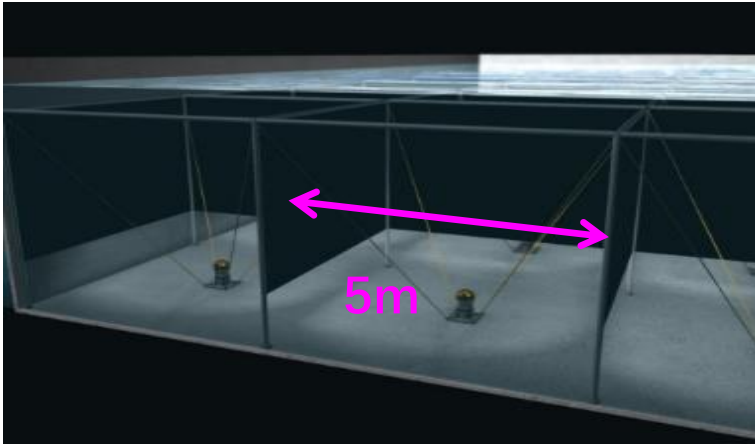


1.3 km²



WFCTA

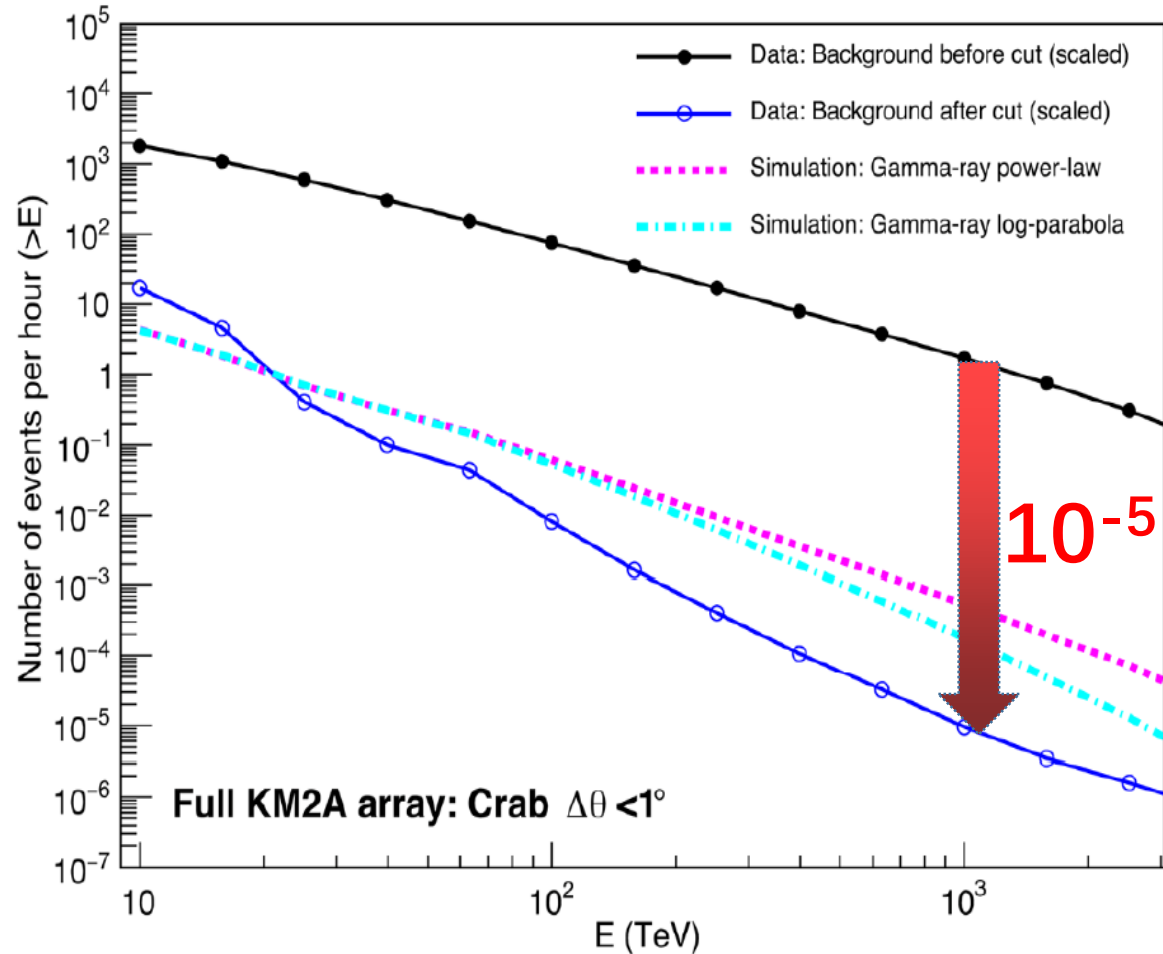
18x4.7m²



WCDA

3120x25m²

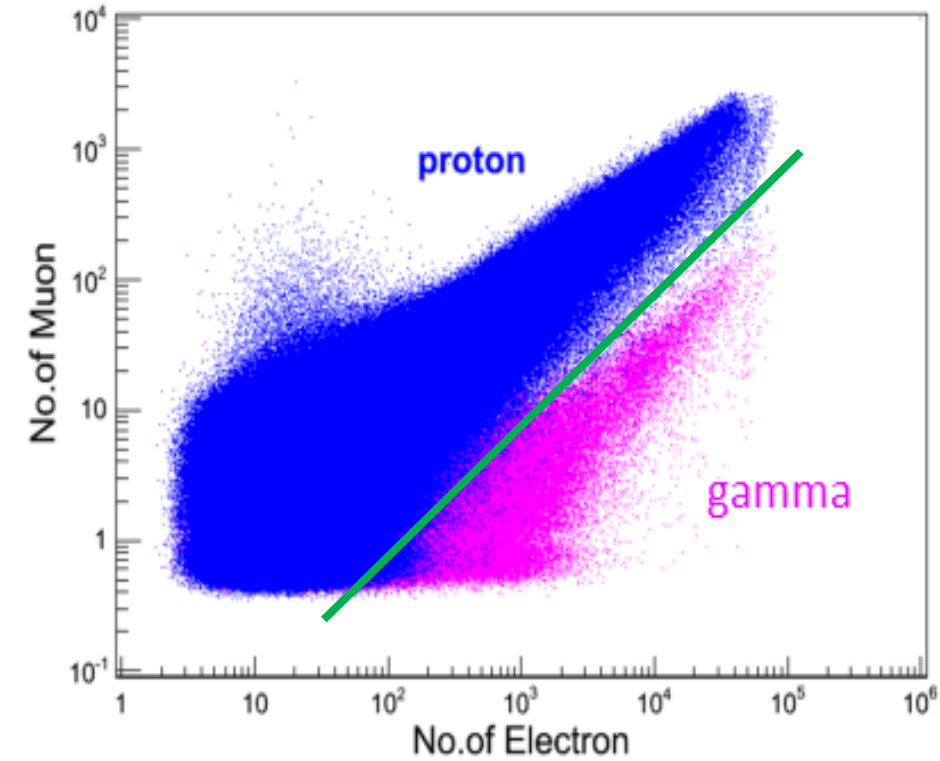
Gamma-ray/cosmic ray discrimination



**Before cut:
CR rate**

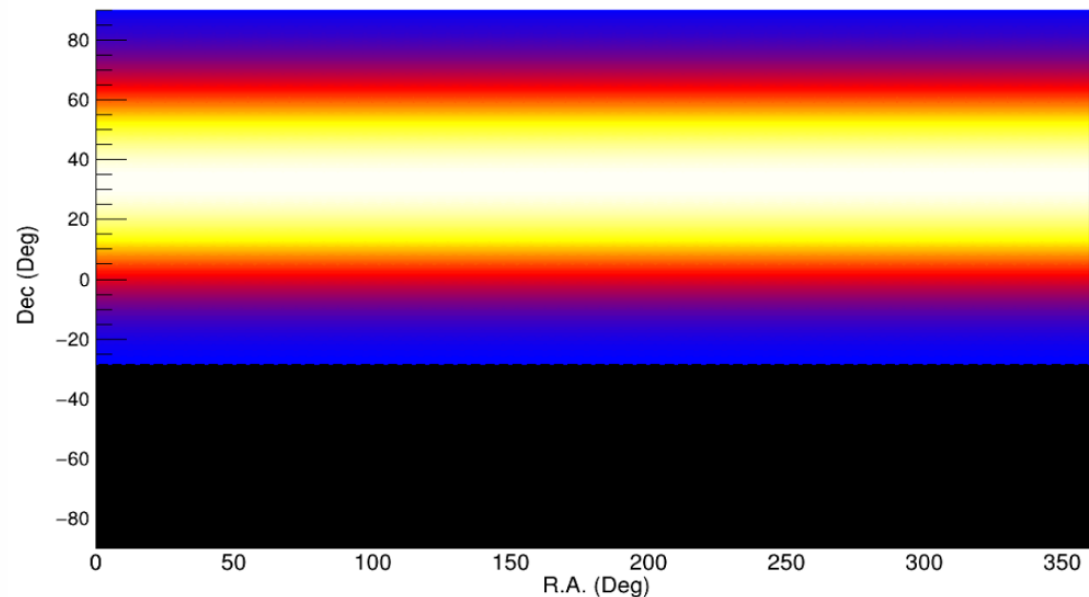
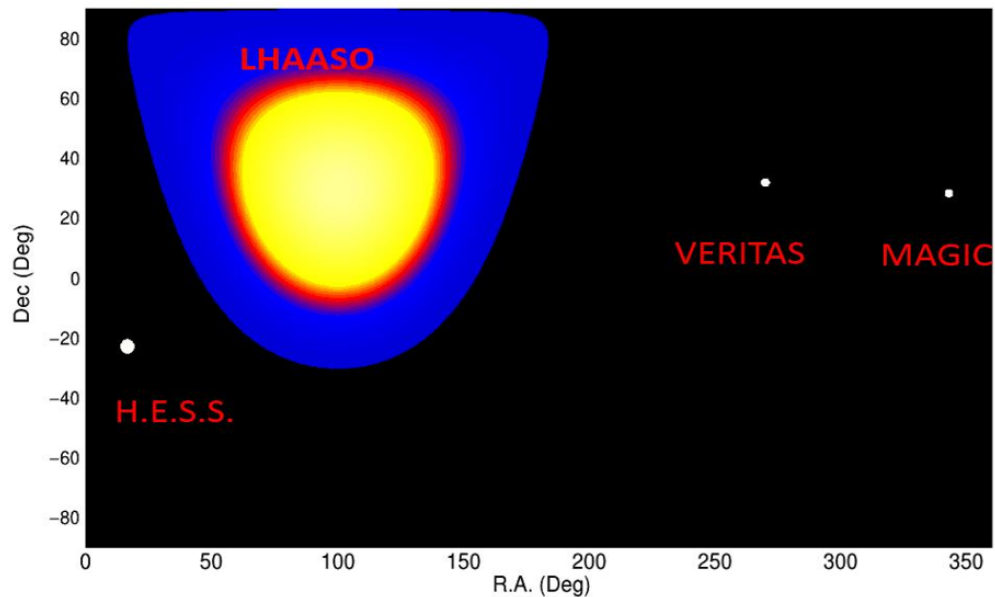
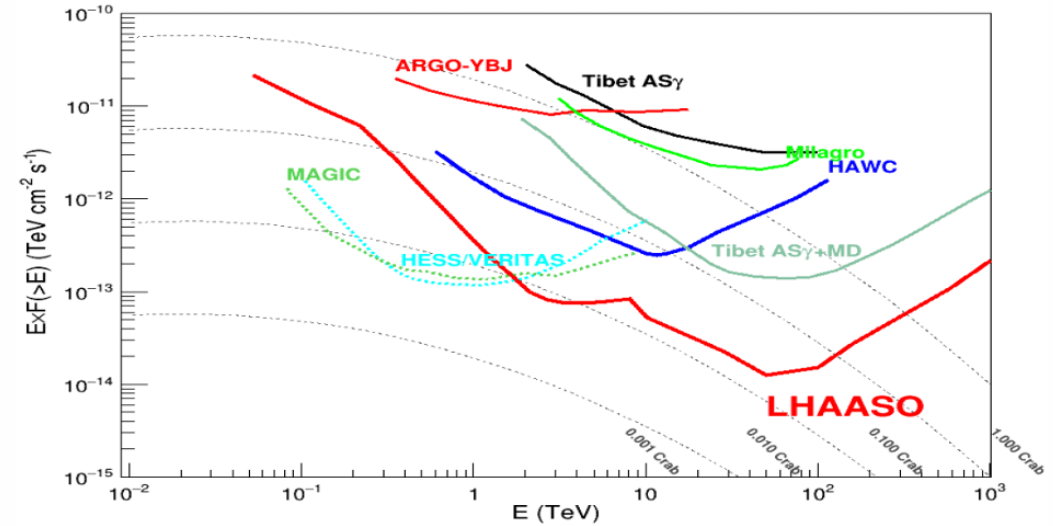
Gamma-ray rate

After cut: CR rate

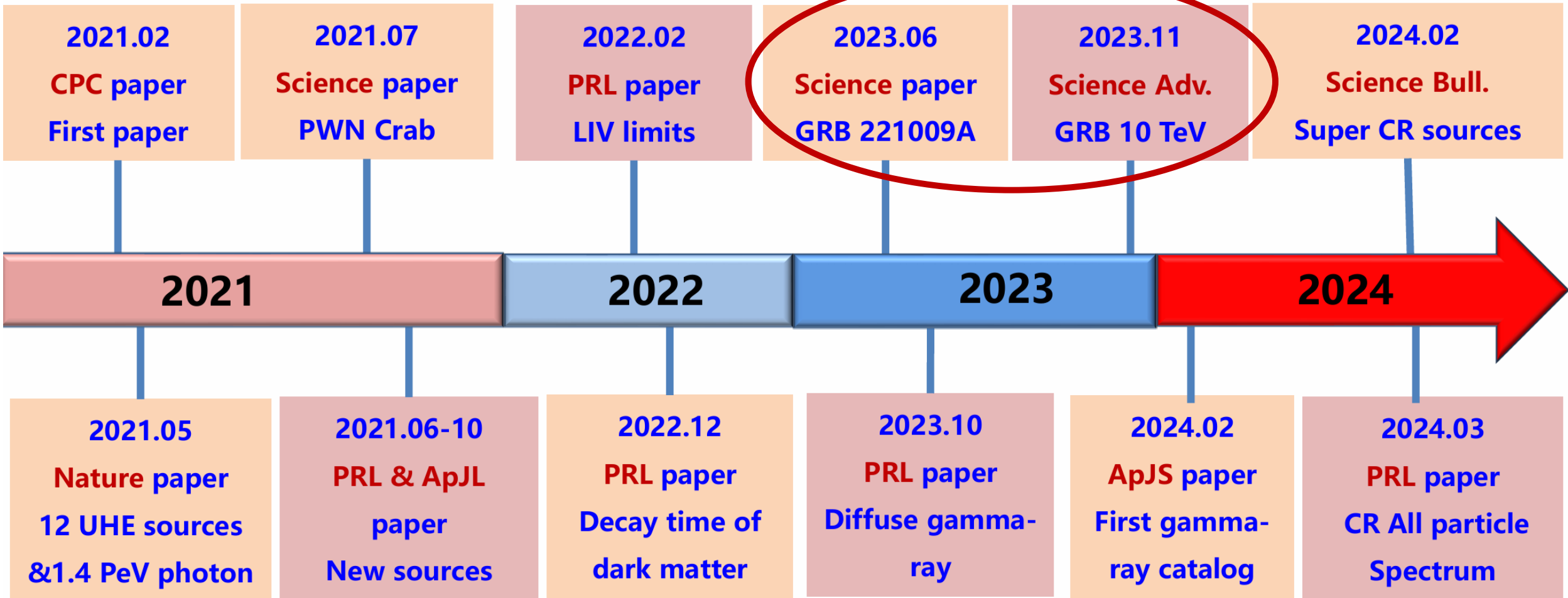


LHAASO for gamma-ray astronomy

- **Features** : Large FOV, Full duty cycle, Wide energy, High sensitivity
- **Important for**: sky survey, extended sources, transient sources

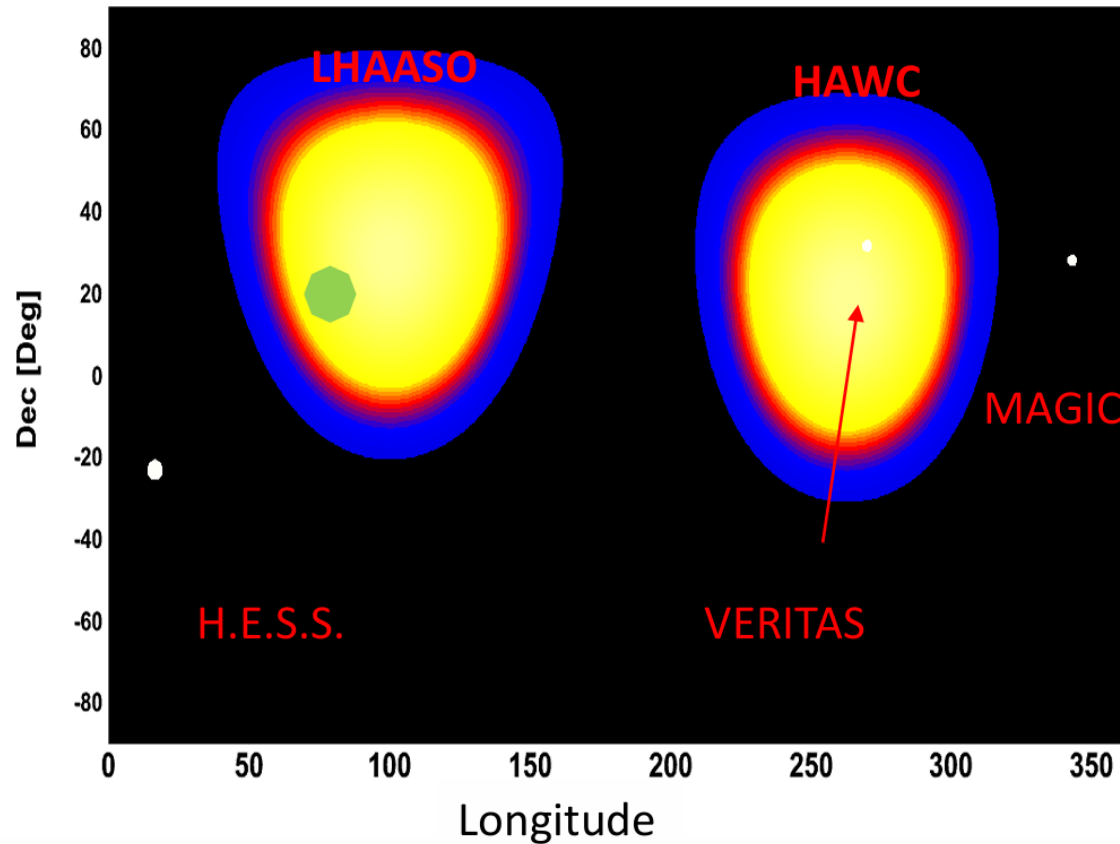


LHAASO important results

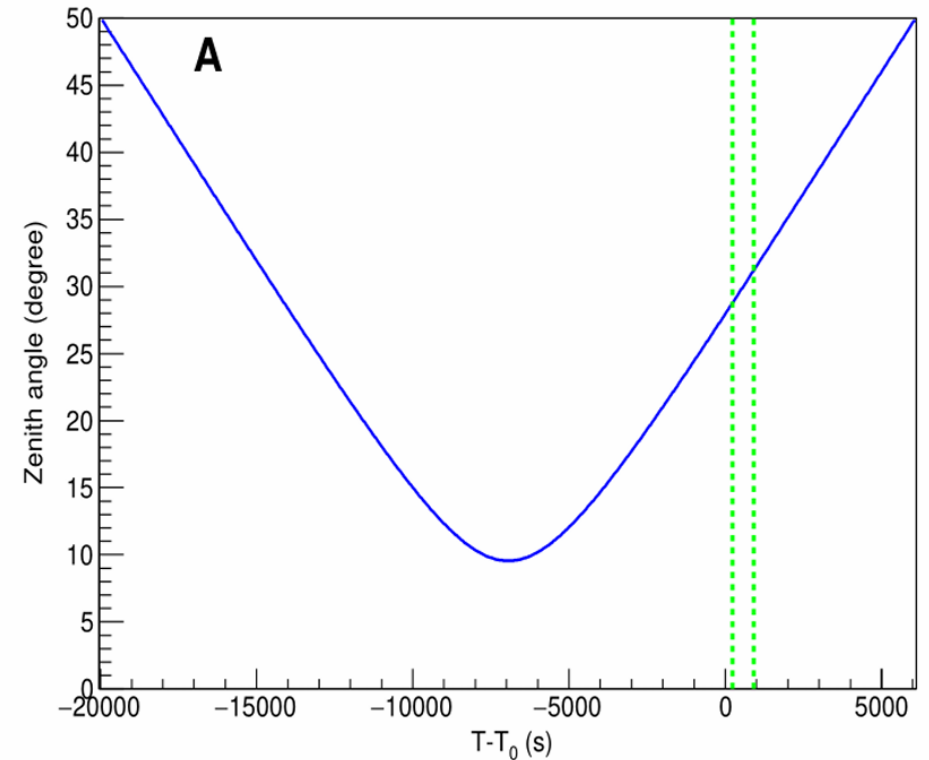


GRB 221009A @FOV of LHAASO

GRB 221009A is well observed by LHAASO at a favorite zenith angle!

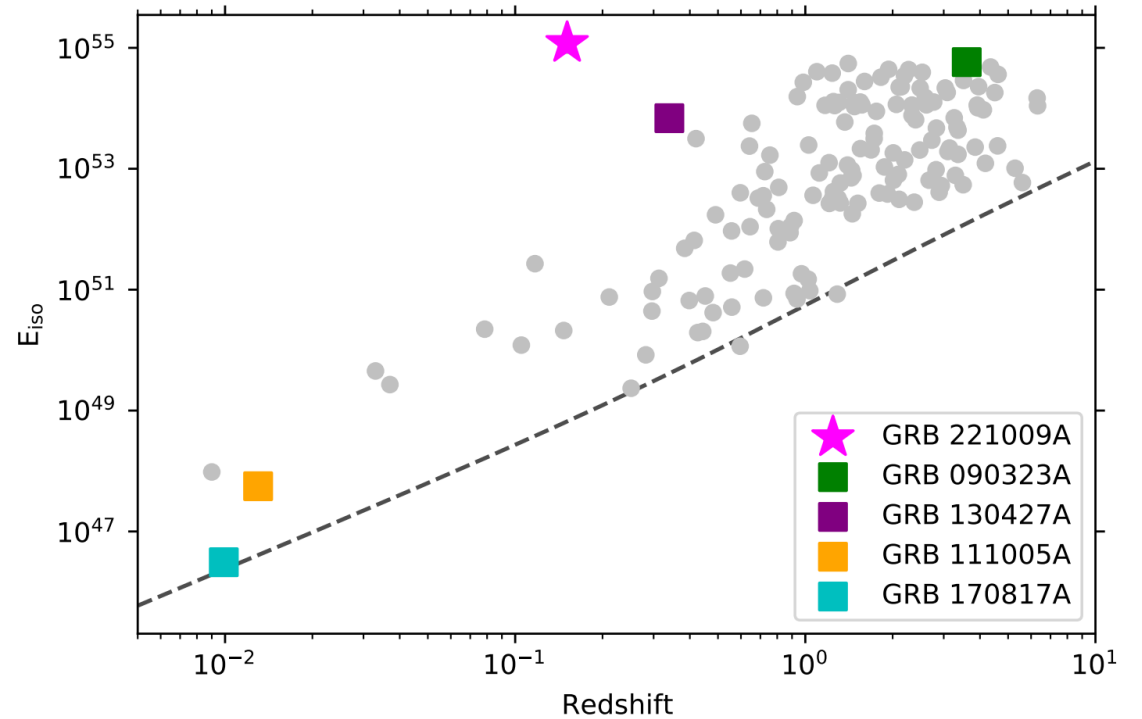
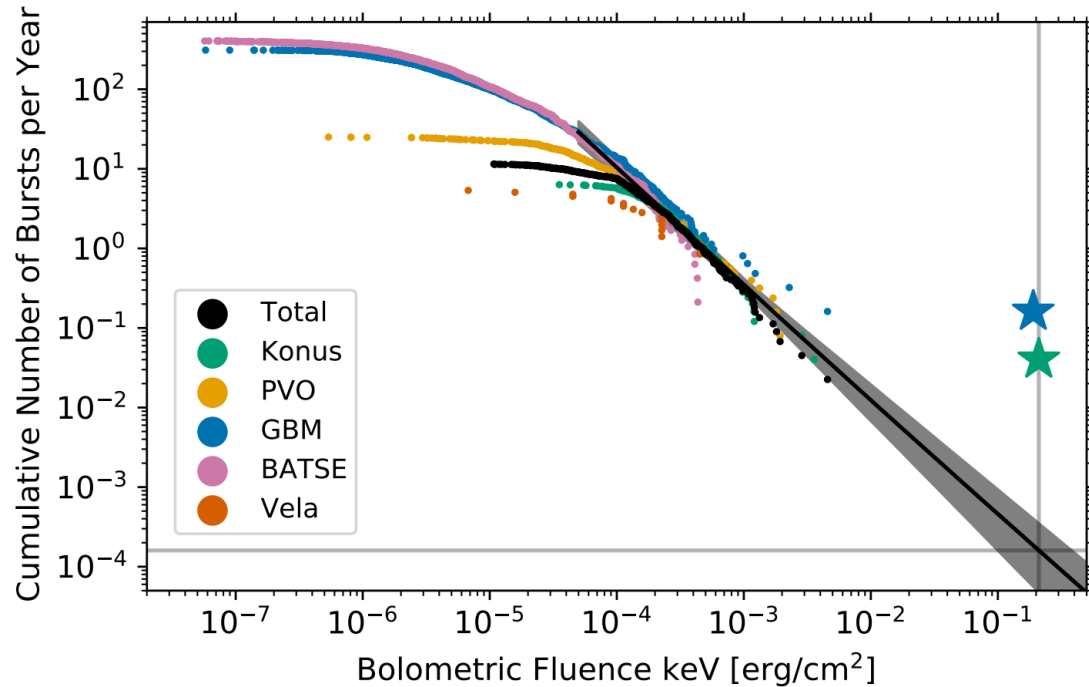


FOV



Zenith angle vs Time

GRB 221009A: A very rare event



Fluence: $>5 \times 10^{-2} \text{ erg/cm}^2$

$R_{\text{GRB}} \leq 6.1 \times 10^{-4} \text{ Gpc}^{-3} \text{ yr}^{-1}$

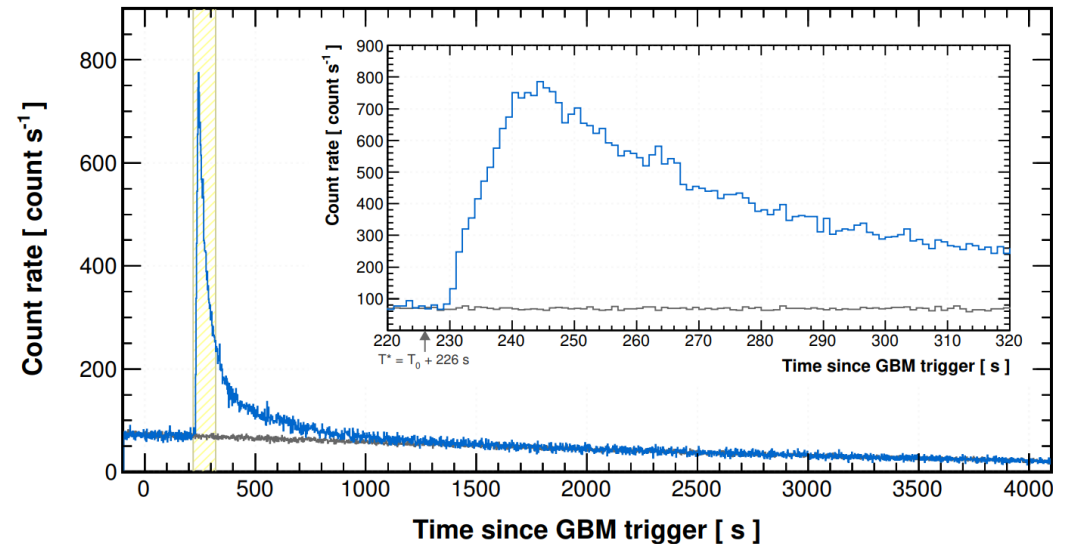
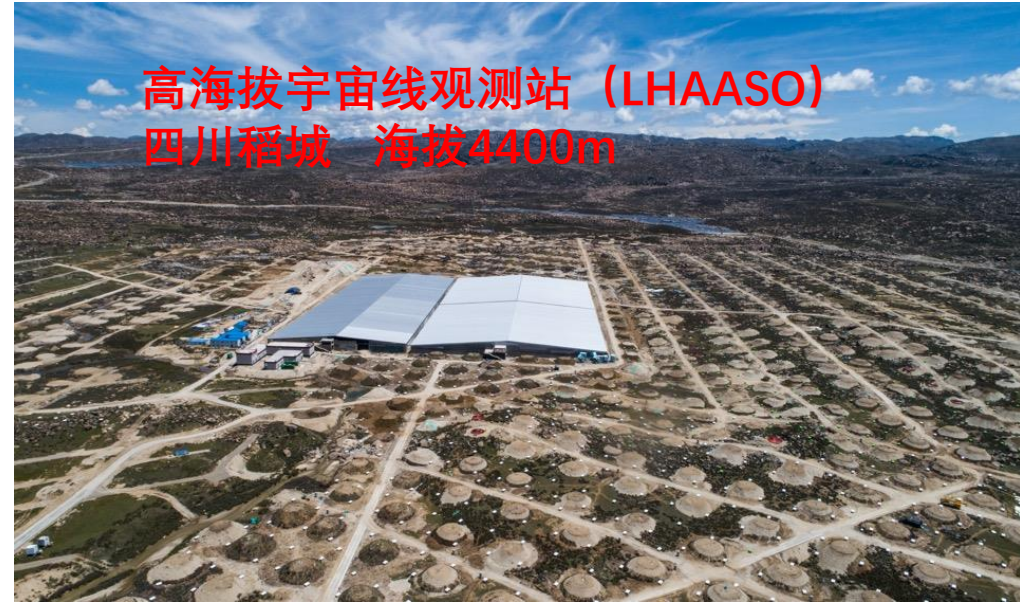
$z=0.151$ volume $\sim 1 \text{ Gpc}^3$

$R < 10^{-3} \text{ yr}$

Buns et al. 2023

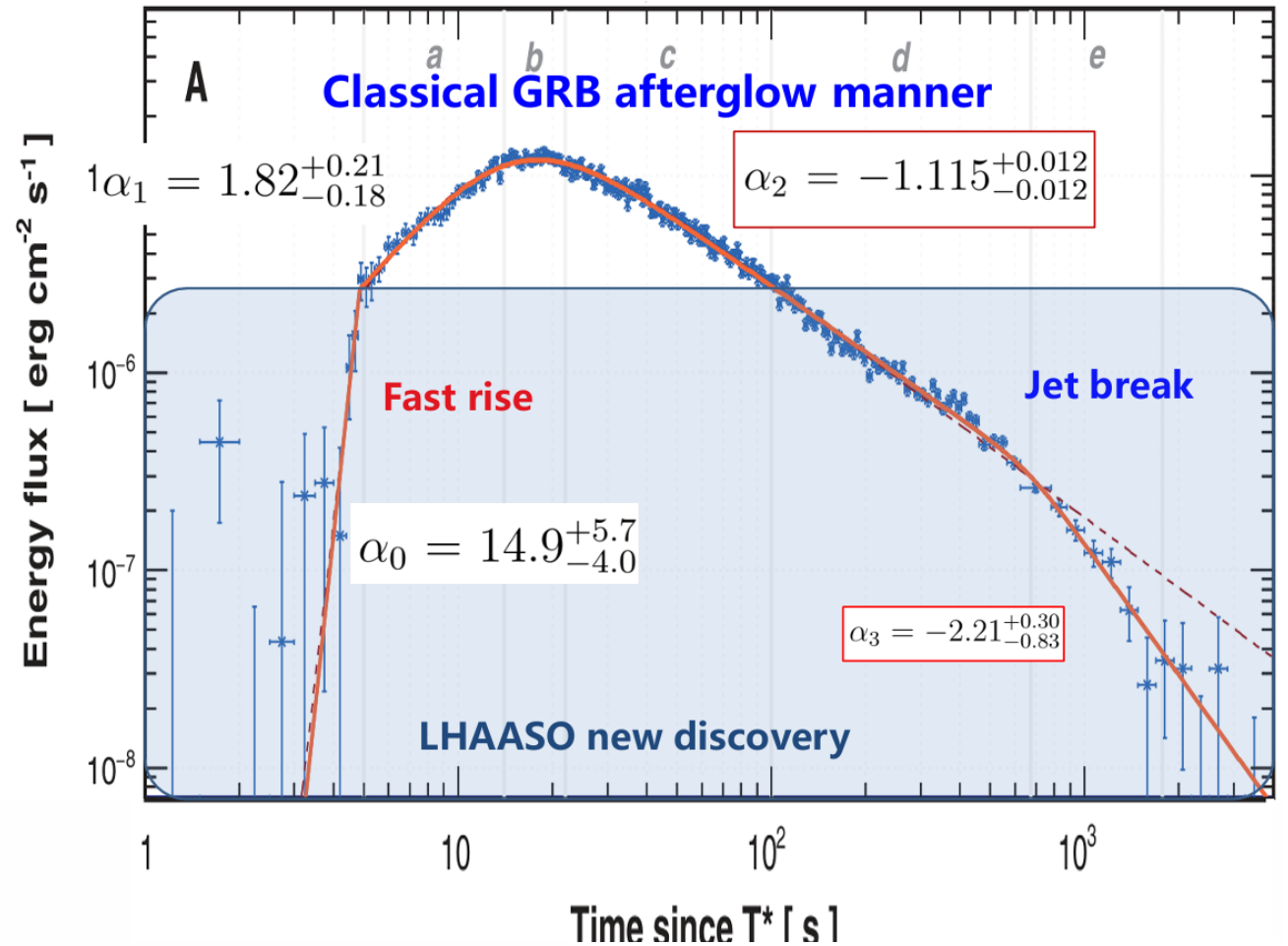
GRB221009 at LHAASO-WCDA

- High statistics: **>60,000 photons** above 0.2TeV (LHAASO-WCDA)
- The whole process of onset and fade of TeV afterglow is recorded. The onset of TeV afterglow is observed for the first time.
- It is also the first time that a GRB is seen by an extensive air shower detector



4-segement Power-law

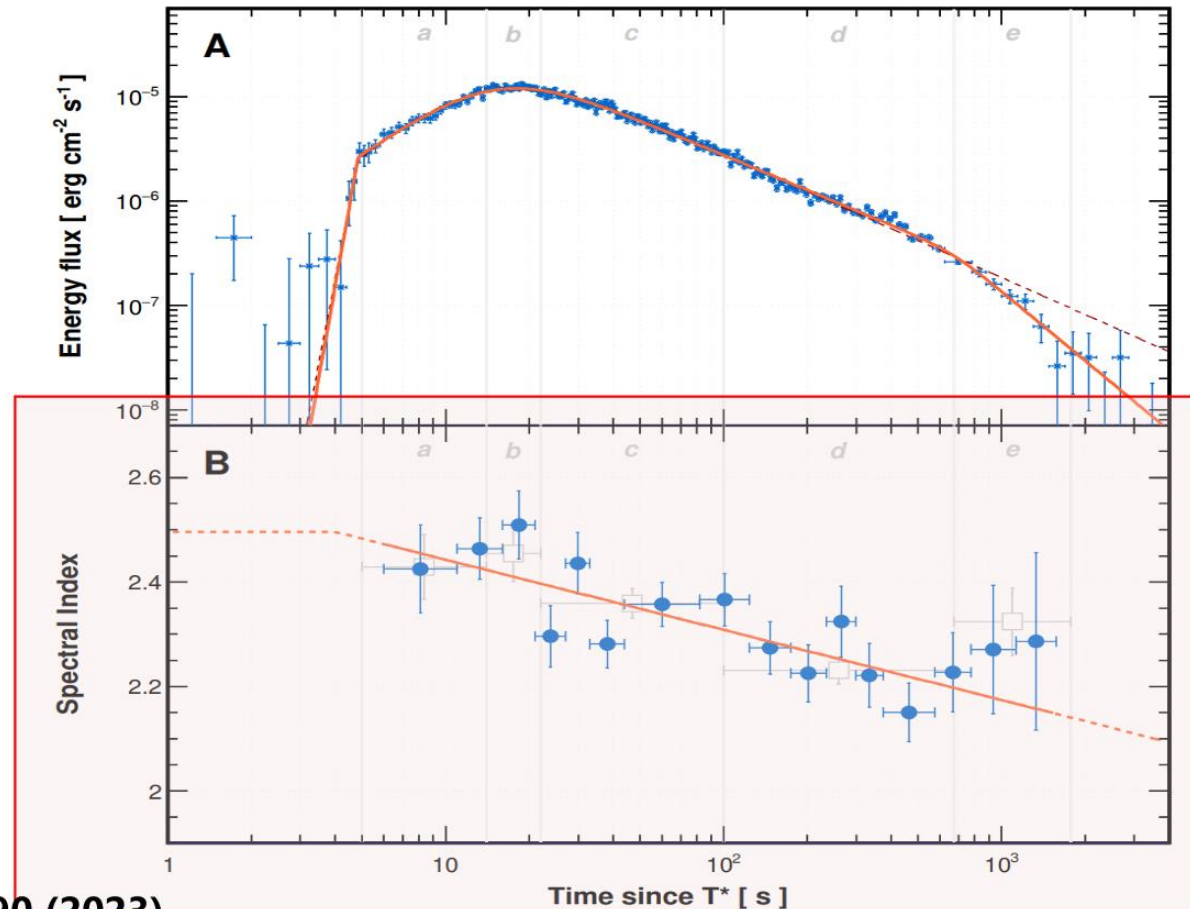
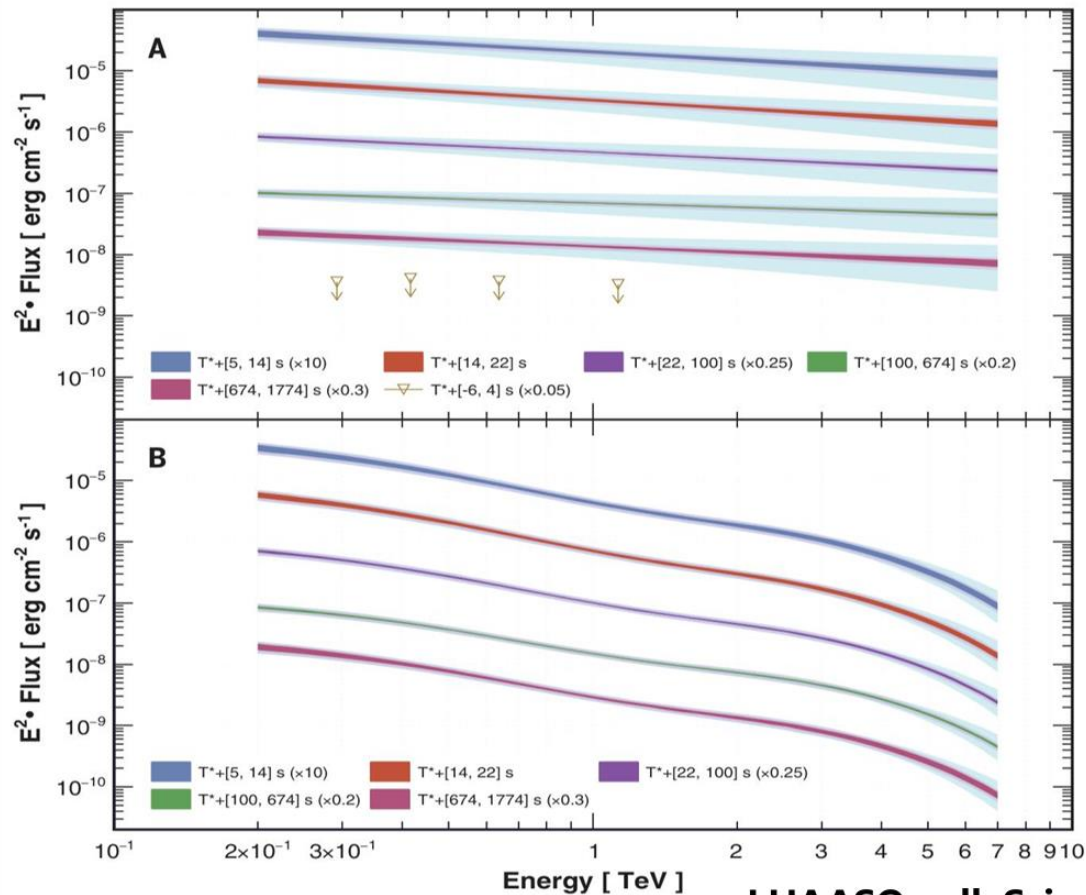
- **Unusual Fast rise:** energy injection ?
- **Slow rise:** Favor ISM environment?
- **Peak time:** The bulk Lorentz factor of **440**.
- **Slow decay:** Electron SED index -2.1
- **Fast decay:** A jet break at the earliest time!



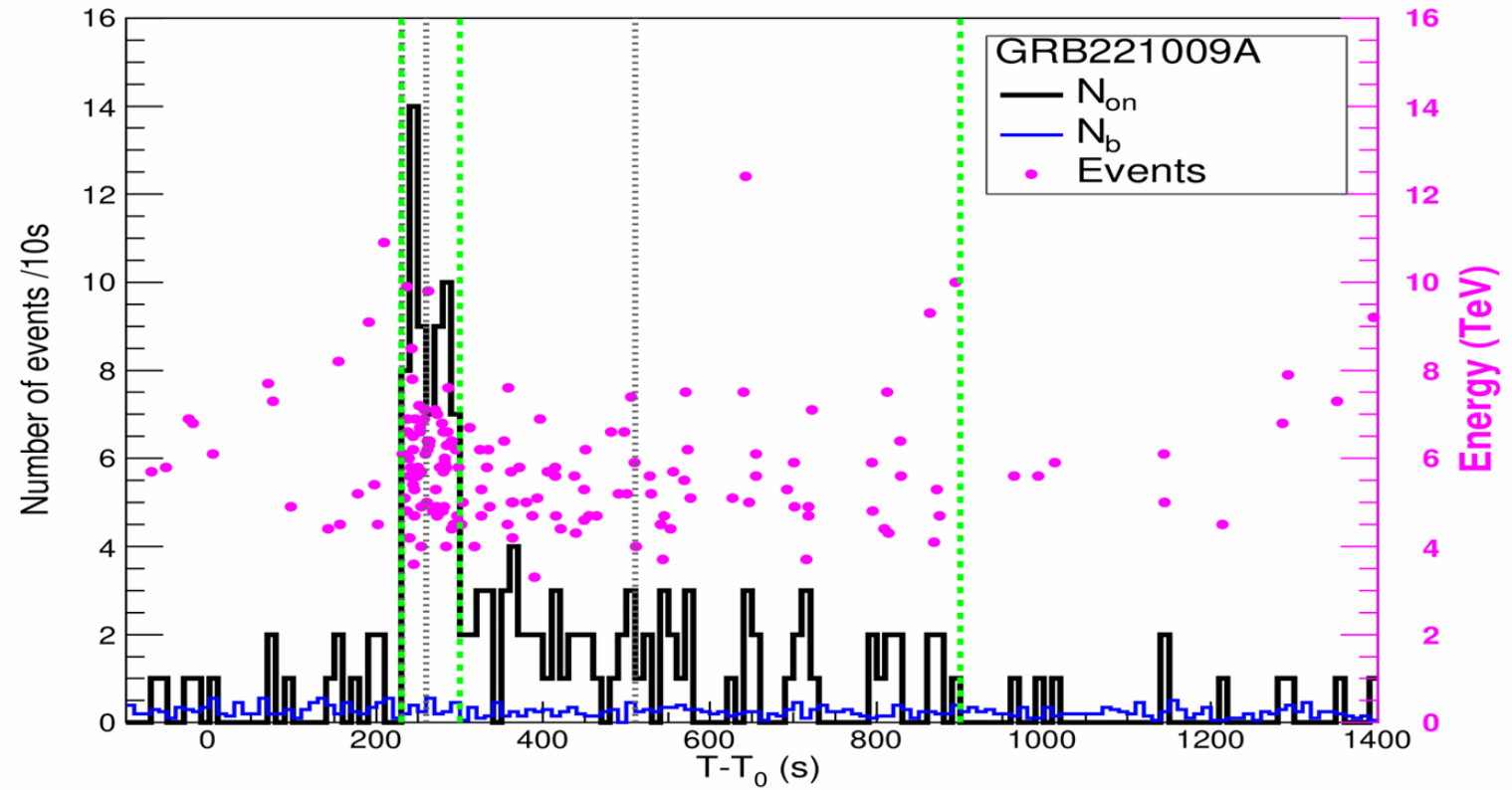
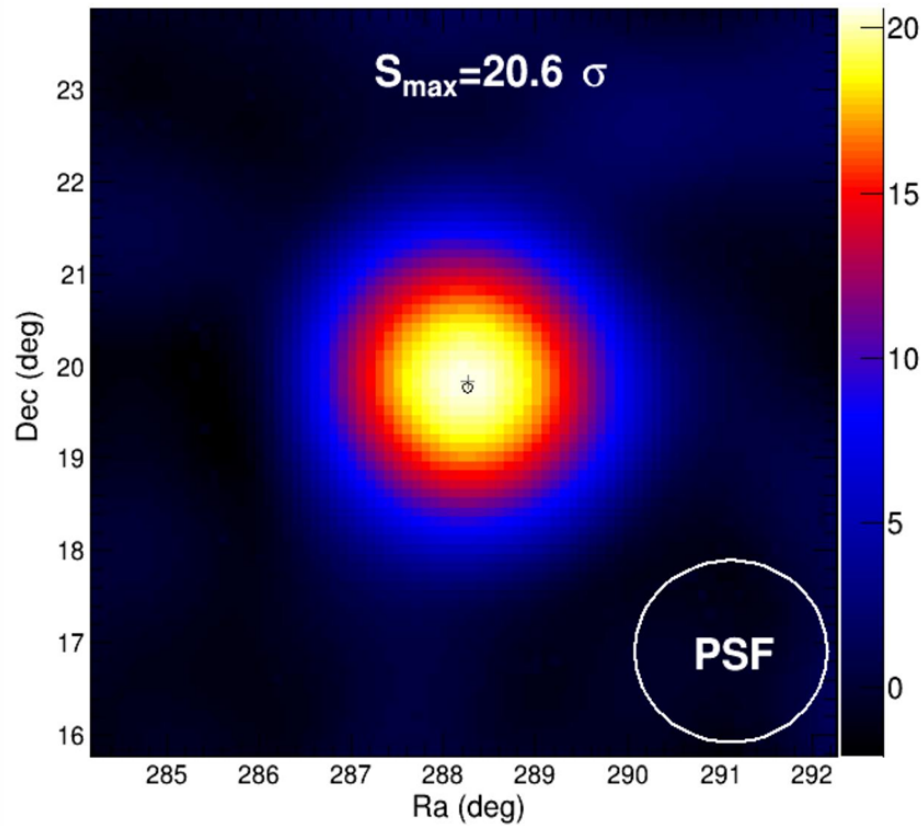
LHAASO coll. Science, 380:1390 (2023)

Unexpected SED evolution

- The SED become harder as time increasing. This is unexpected from standard afterglow model!

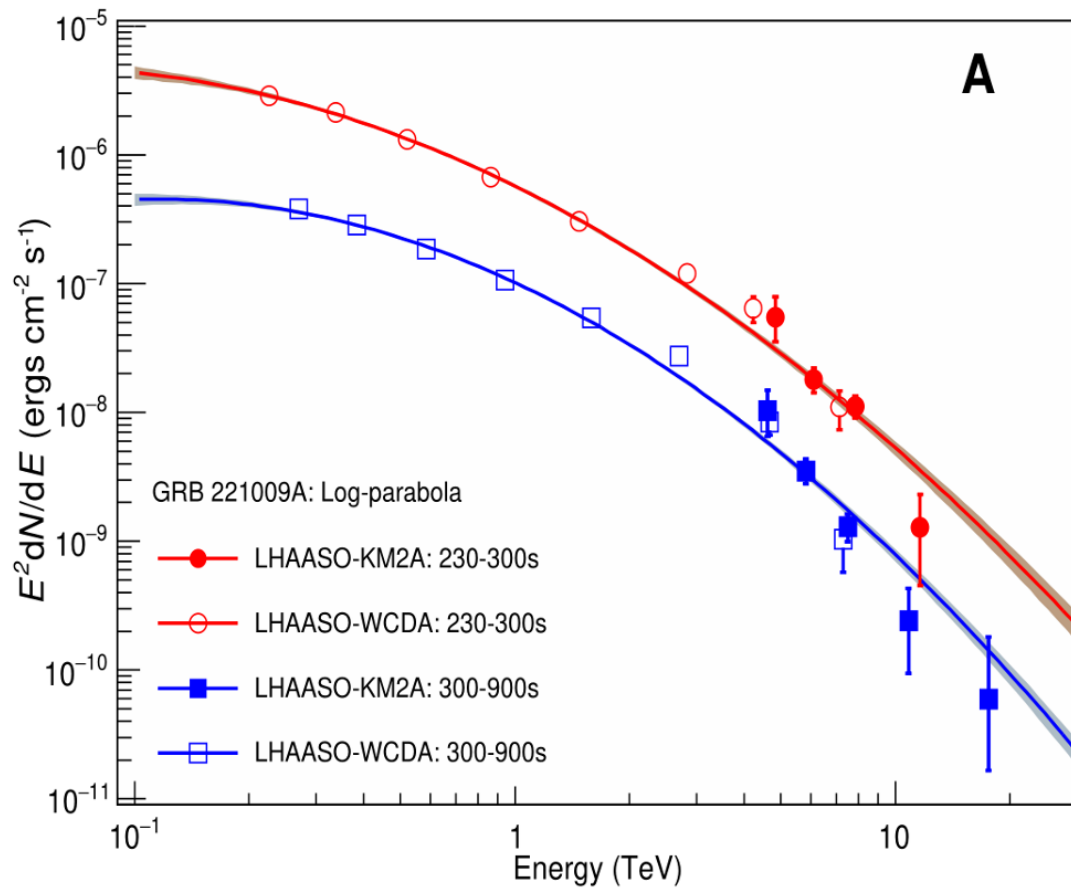


KM2A at higher energies

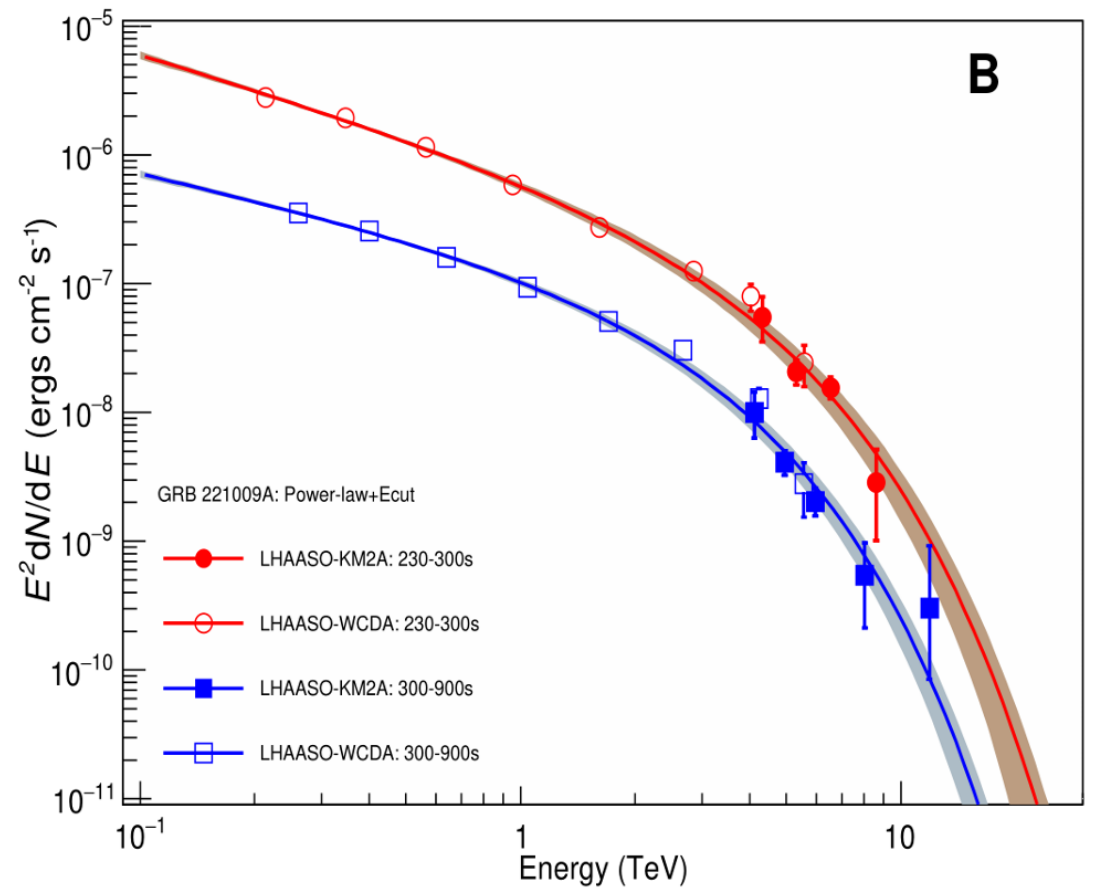


WCDA+KM2A SED (observed)

SED function: log-parabola

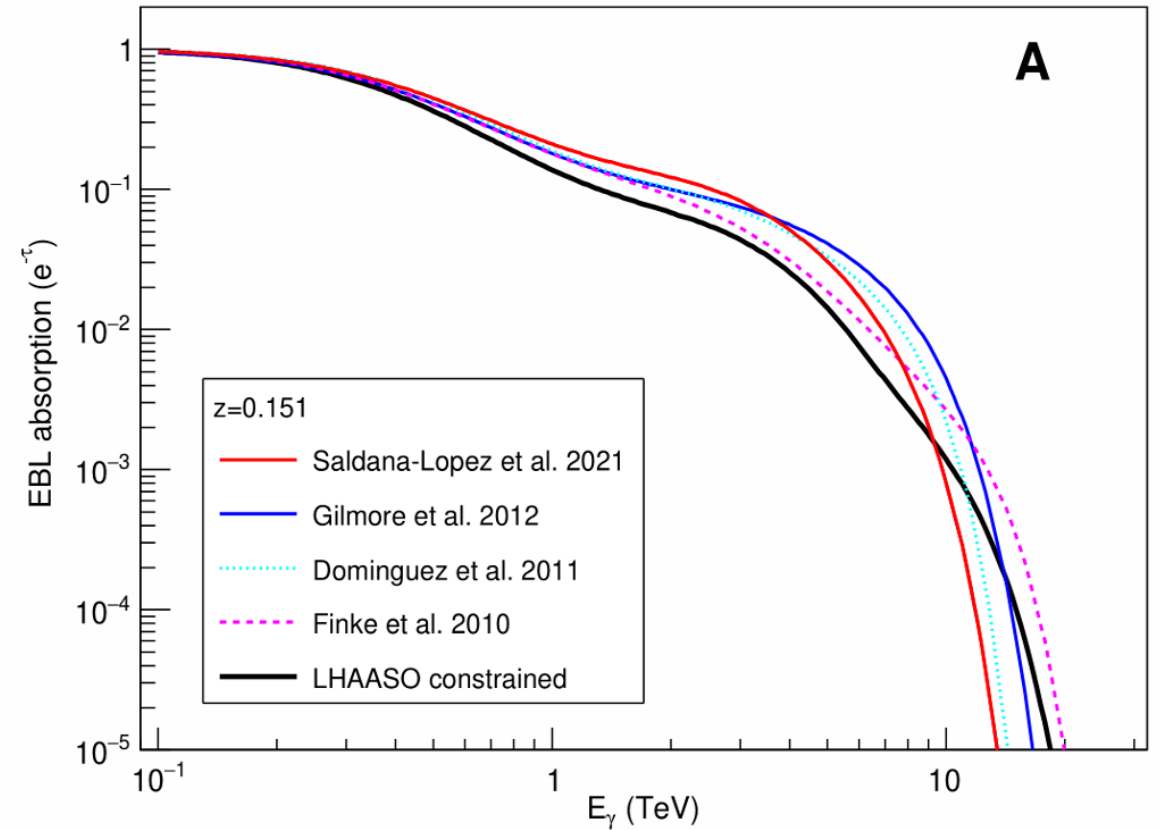
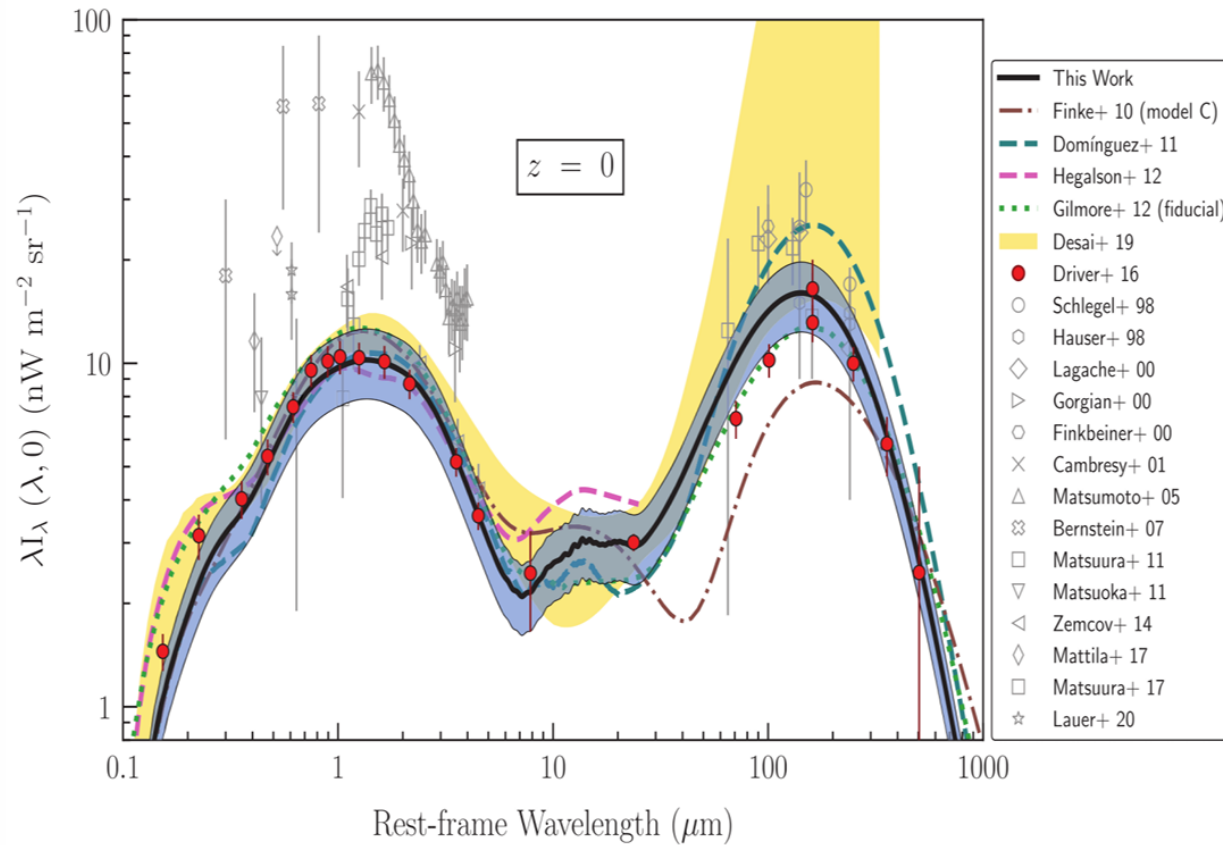


SED function: Power-law+Ecut



EBL absorption

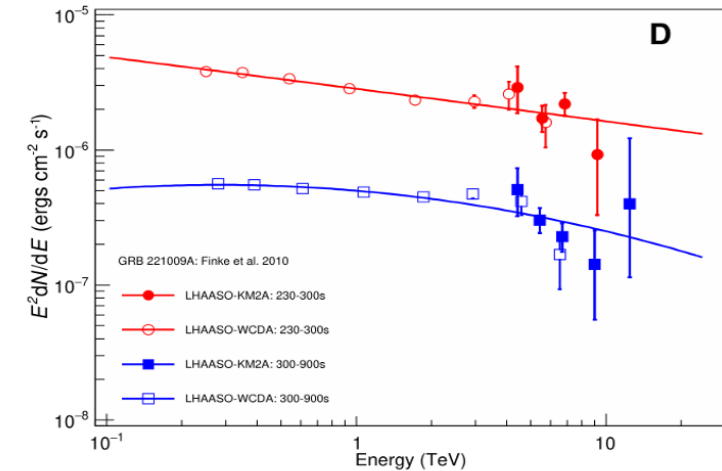
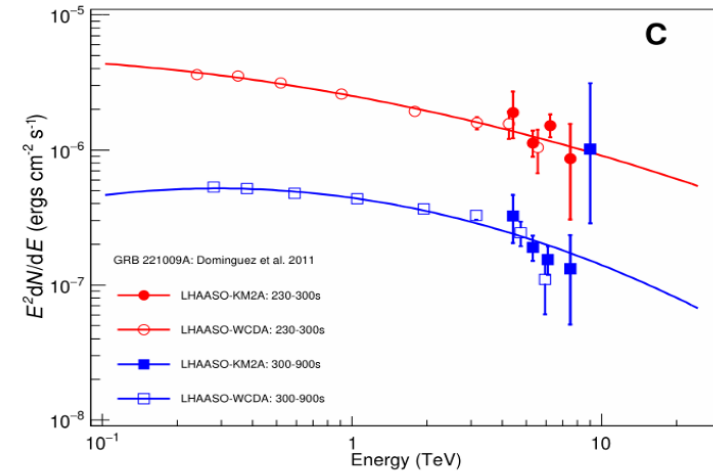
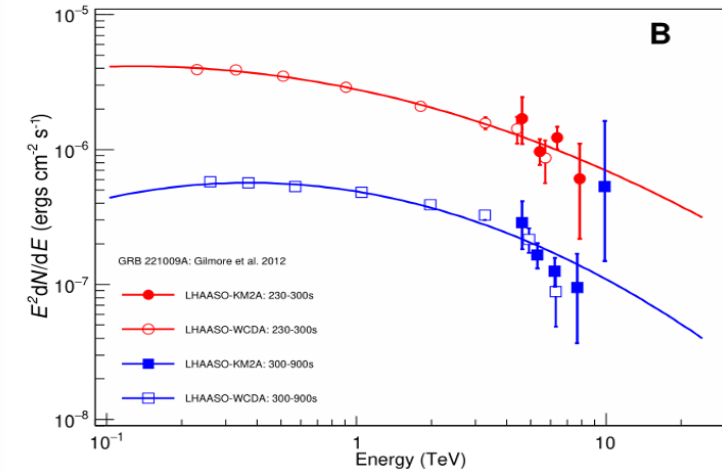
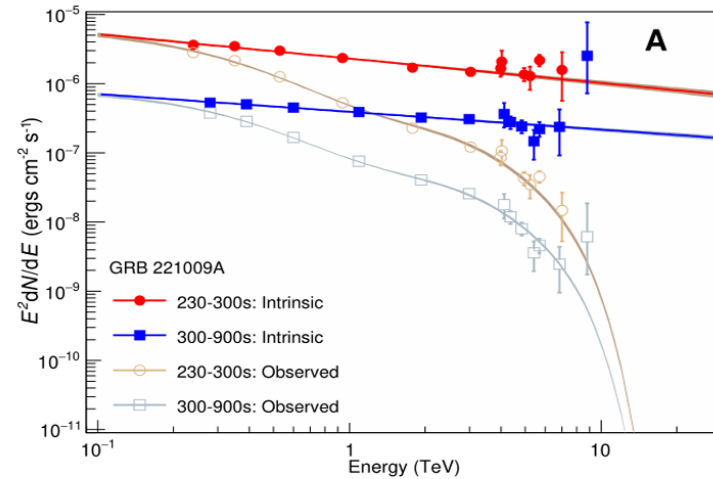
Alberto Saldana-Lopez^{b, 1,2*}, Alberto Domínguez^{b, 2*}, Pablo G. Pérez-González^{b, 3}, Justin Finke^{b, 4},
Marco Ajello^{b, 5}, Joel R. Primack^{b, 6}, Vaidehi S. Paliya^{b, 7} and Abhishek Desai^{b, 8}



Saldana-Lopez et al. 2021

WCDA+KM2A SED (EBL corrected)

- Intrinsic SED using different EBL models



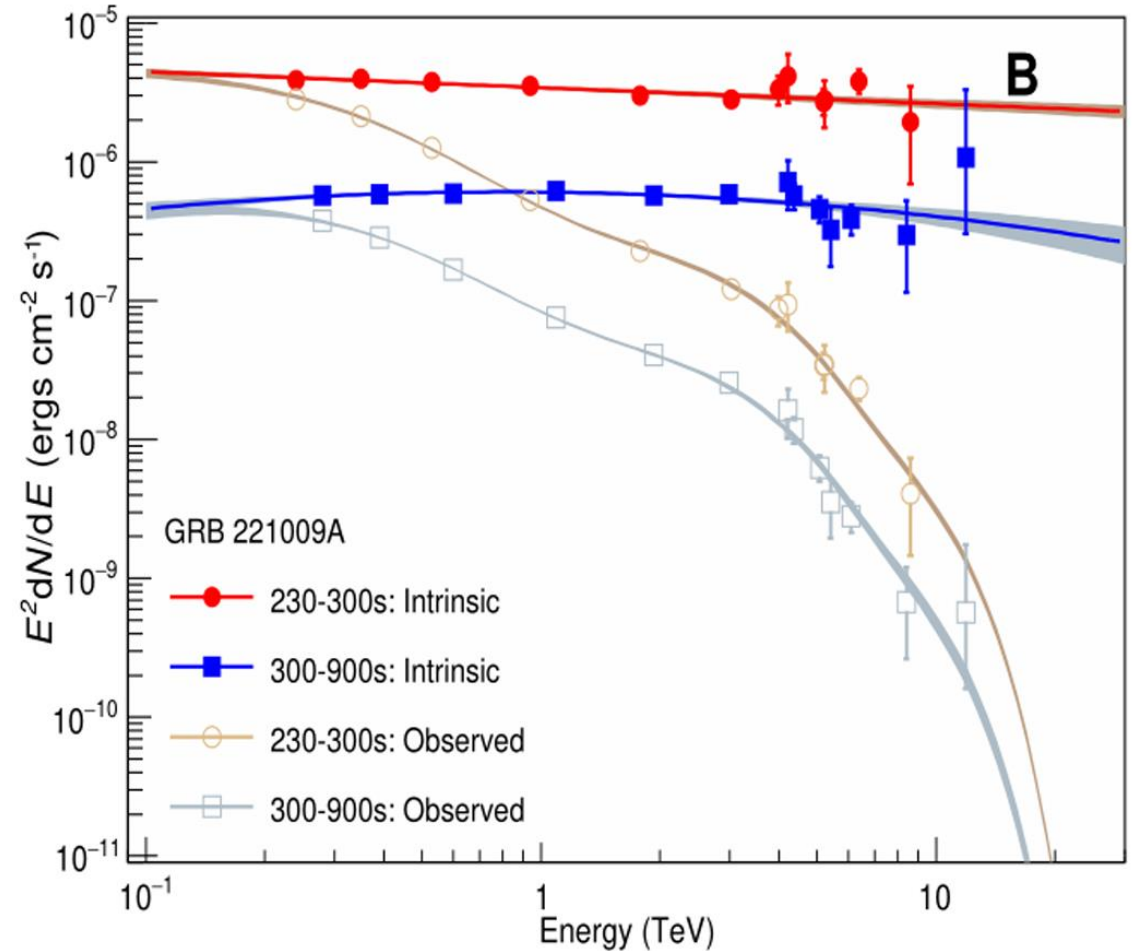
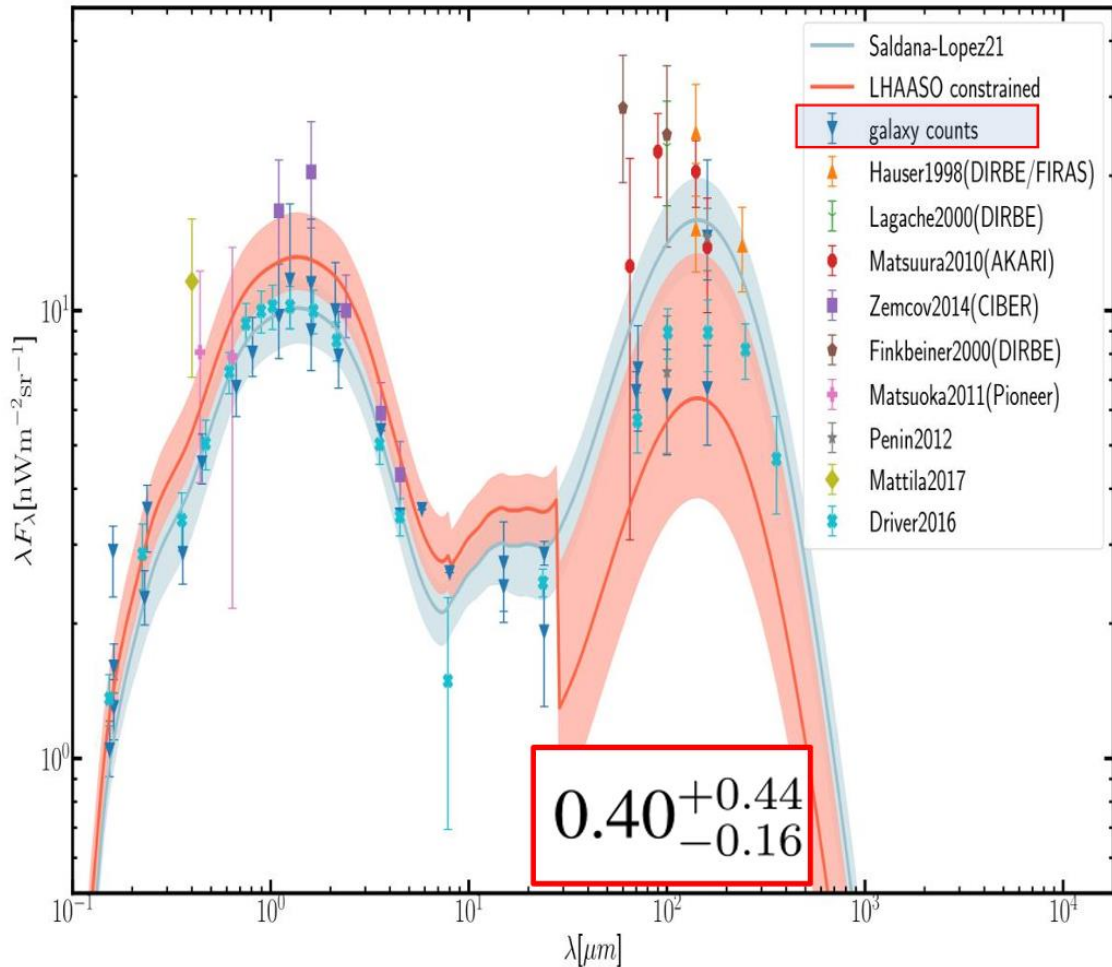
Implications of the LHAASO observation

- Constrain the EBL models
- Possible new physics scenarios
 - axion
 - LIV

LHAASO coll. Science Advances,9: eadj2778 (2023)

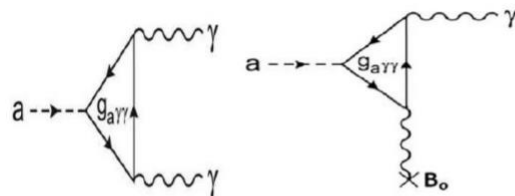
Constraints on EBL distribution

$\lambda < 8\mu\text{m}$, $8\mu\text{m} < \lambda < 28\mu\text{m}$, $\lambda > 28\mu\text{m}$



Axion and axion-like particles

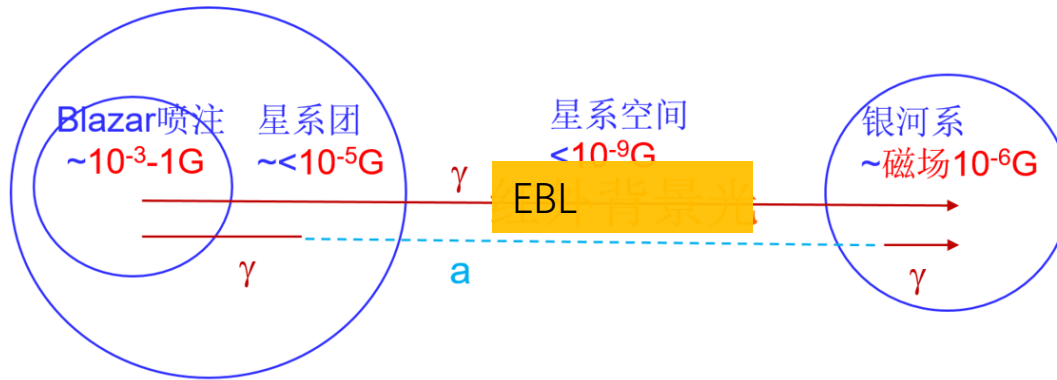
- Axion is introduced to solve the strong CP problems of the SM. It is an ideal cold dark matter candidate
- Axion couples with two photons
- In external magnetic field axion-gamma oscillates into each other



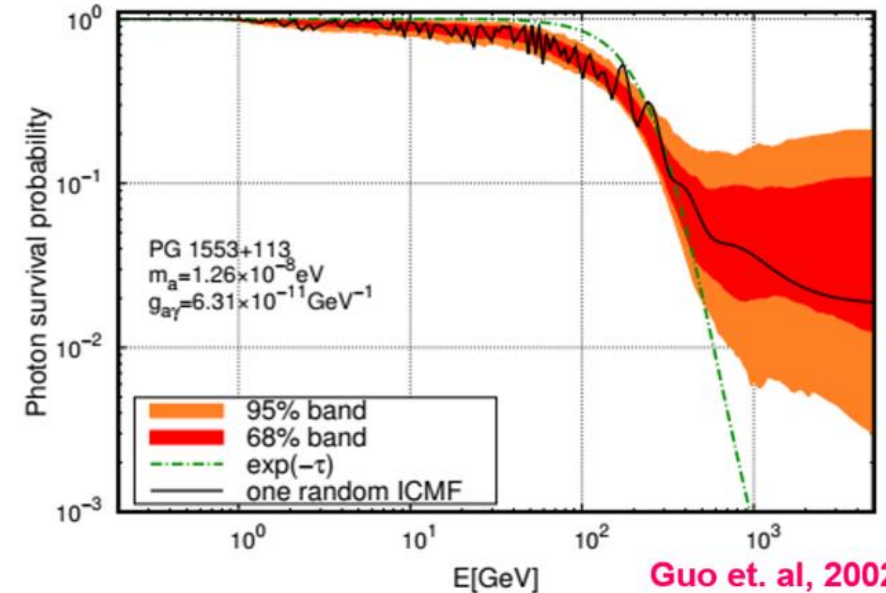
$$\mathcal{L} = -\frac{1}{4}F_{\mu\nu}^2 + \frac{1}{2}(\partial_\mu a \partial^\mu a - m^2 a^2) + \frac{g_{a\gamma}}{4} a F_{\mu\nu} \tilde{F}^{\mu\nu} ,$$

gamma-axion oscillation

- Oscillation between axion-gamma evade the absorption by EBL



- The gamma ray spectrum is modified



Best fit of axion is not significant

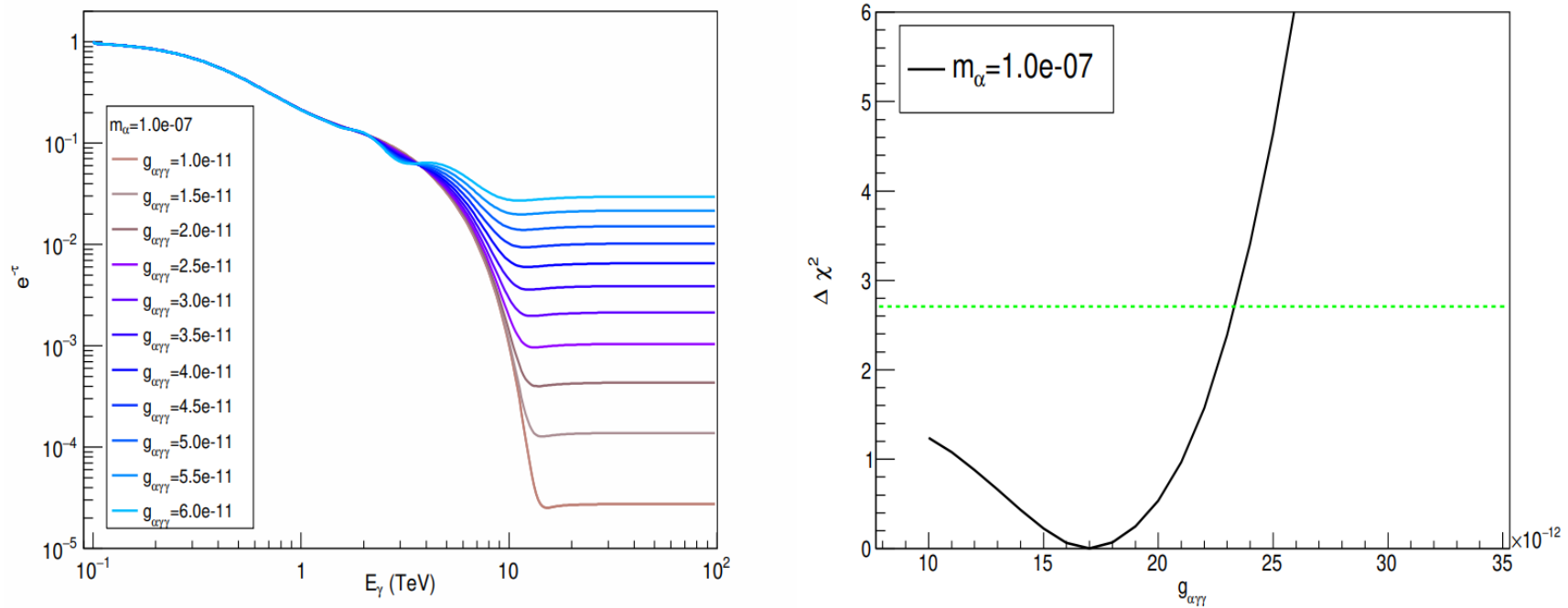
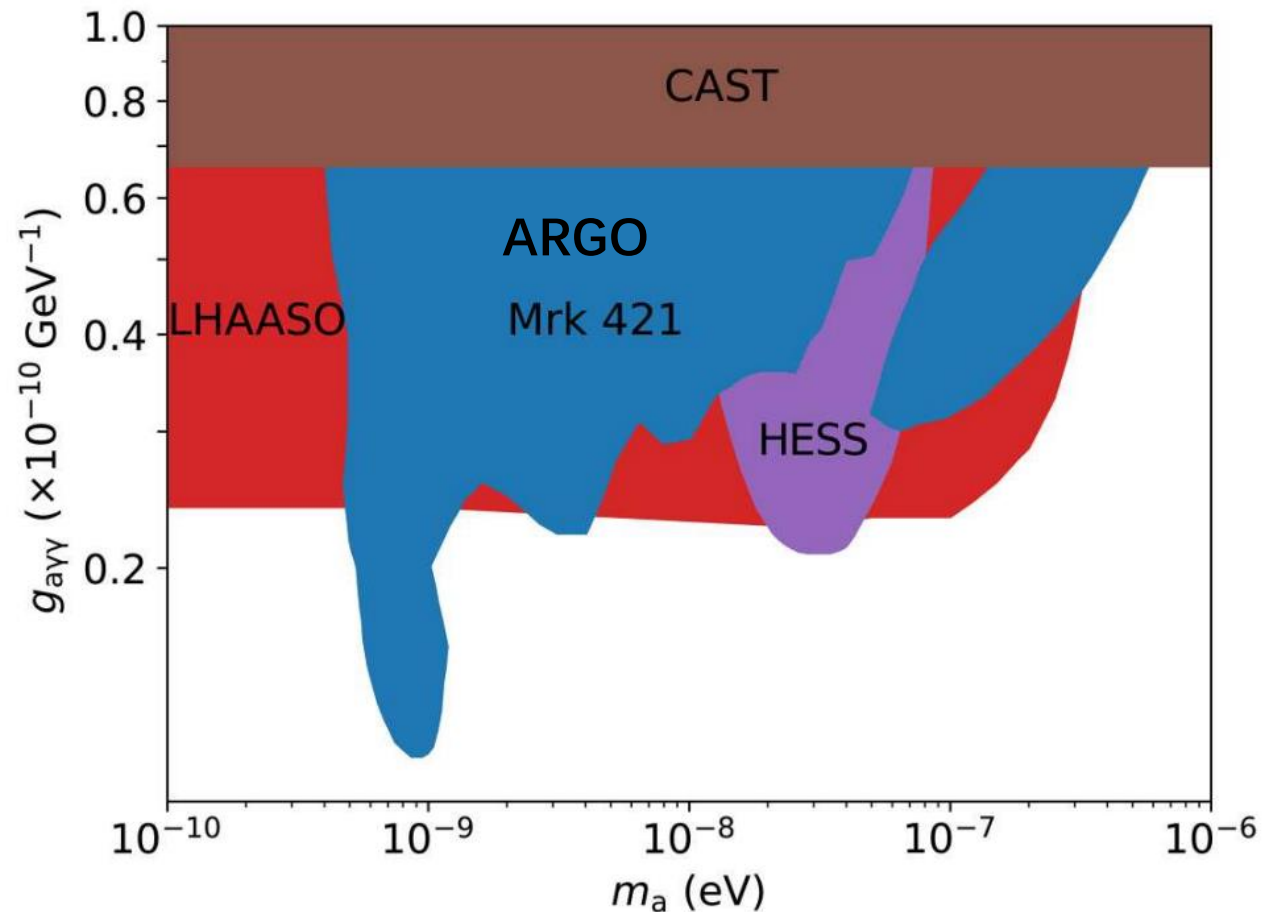
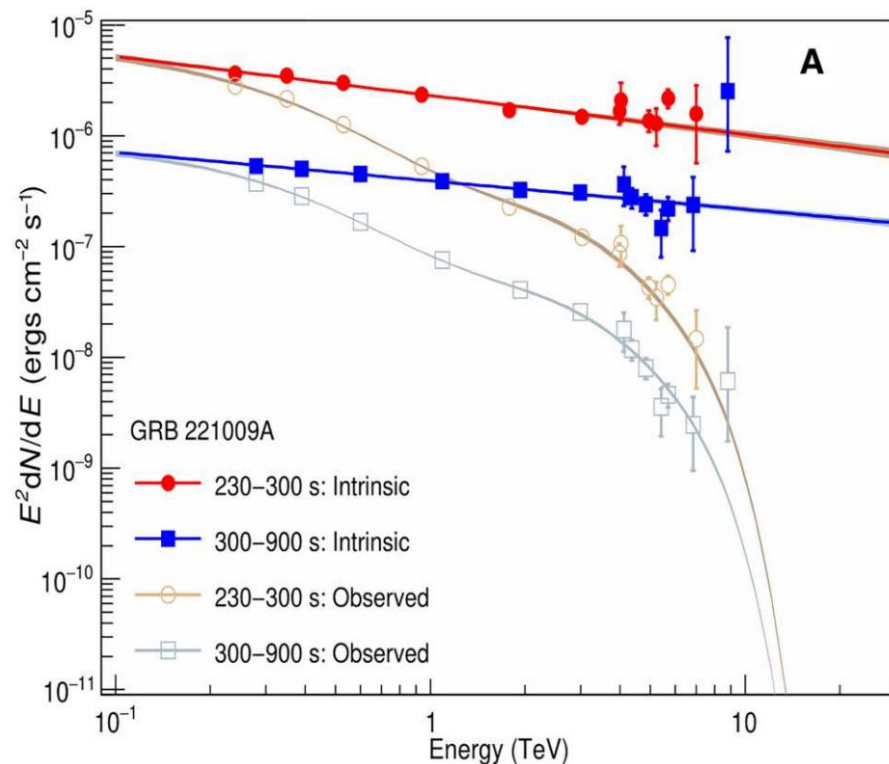


Figure S2: **The EBL absorption and the χ^2 of spectral fitting taking into account the ALP oscillation.** Panel A shows EBL absorption models for very high-energy gamma-rays from a redshift of $z = 0.151$, taking into account the oscillation between gamma-rays and ALPs assuming $m_a = 10^{-7}$ eV and $g_{a\gamma} = (1 \text{ to } 6) \times 10^{-11}$ GeV $^{-1}$. The EBL model used is Saldana et al. 2021. Panel B shows $\Delta\chi^2$ relative to the minimum that fits the spectral energy distribution data as a function of the ALP $g_{a\gamma}$ for $m_a = 10^{-7}$ eV. The line indicates $\Delta\chi^2 = 2.71$ used to define the upper limit on $g_{a\gamma}$.

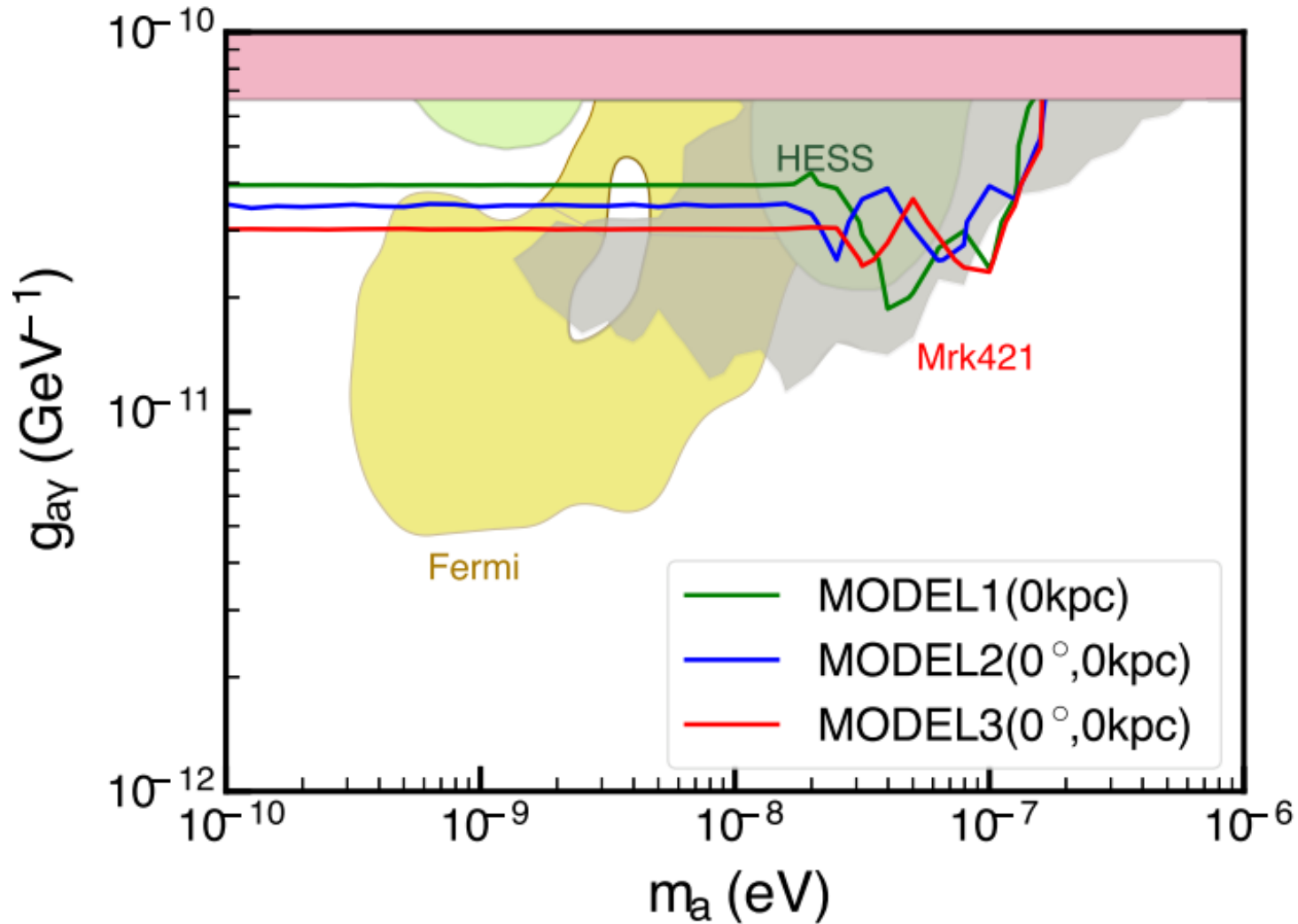
A stringent constraint is set on axion coupling

LHAASO coll. 2023 (Science adv. 9, 2778)

- Axion significance $< 2\sigma$, we give constraints on axion coupling



In comparison with other constraints

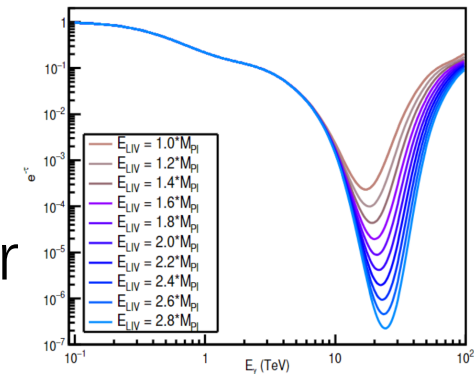


Gao, BXJ, Yao, Yin,
JCAP01(2024)026

Kinetics with LIV $E^2 = p^2 c^2 *(1 + a_1(pc/ M_{pl} c^2) + a_2(pc/ M_{pl} c^2)^2 + \dots)$

- A free photon in vacuum is stable in LI; For LIV, if the effective mass of a photon $E_\gamma^2 - p_\gamma^2 = \frac{p^{n+2}}{E_{LIV}^n} = m_{\gamma,eff}^2$ is greater than a pair of e+e-, the photon decay $\gamma \rightarrow e+e-$ very fast and leads to a sharp cutoff at the SED

- Change the threshold of an interaction. The threshold of $\gamma\gamma \rightarrow e+e-$ $\epsilon_{thr} = \frac{m_e^2 c^4}{E} + \frac{1}{8} \left(\frac{E}{E_{LIV}} \right) E$ is improved; more transparent for

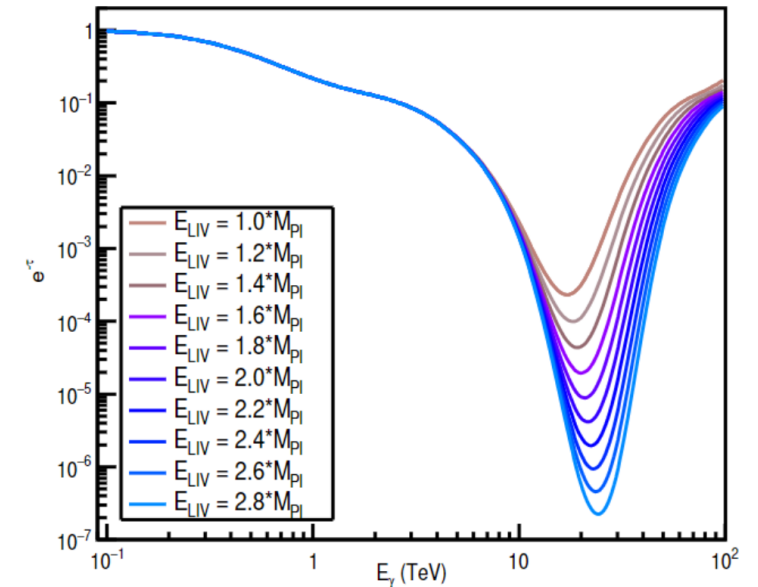
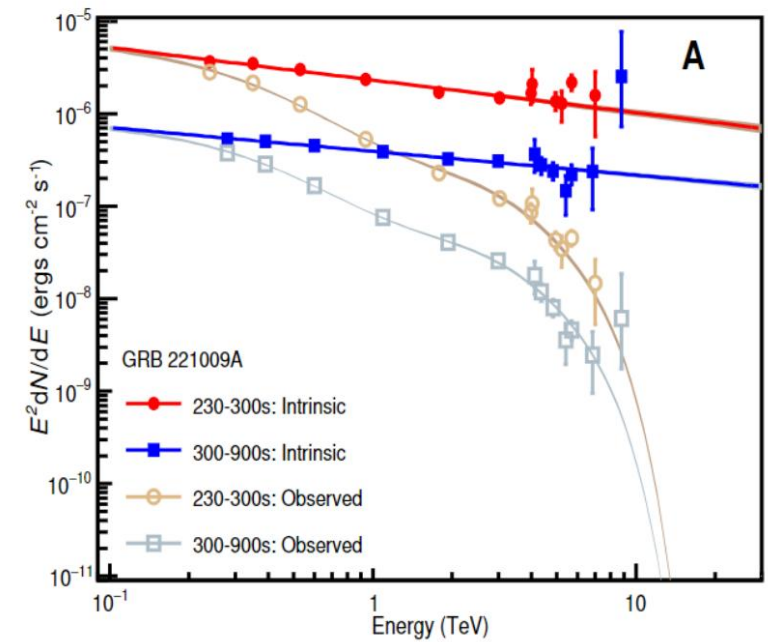


- Energy dependent speed of light at LIV; $v(E) = \frac{\partial \omega}{\partial k} = \frac{\partial E}{\partial p} \approx c \left(1 \pm \frac{1+n}{2} (E/E_{LIV,n})^n \right)$, it leads to time delay for different E from z,
- ... others

$$\Delta t = \frac{\Delta z}{H_0} = \frac{1+n}{2H_0} \left(\frac{E_0}{\xi E_{pl}} \right)^n \int_0^z \frac{(1+z')^n dz'}{\sqrt{\Omega_m (1+z')^3 + \Omega_\Lambda}}$$

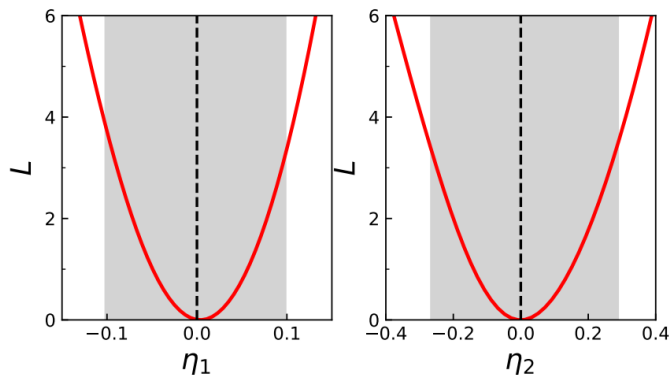
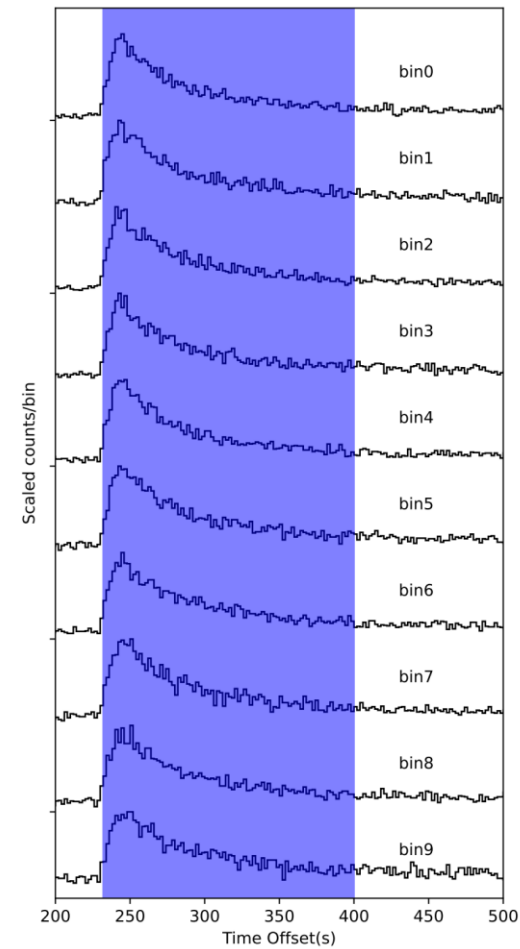
LIV by GRB 221009A

- The intrinsic gamma spectrum shows a bump at the highest energy. It stimulates a lot of interests. LIV is a possible solution which leads to more transparent EBL.
- As the significance is not high. Constraint on LIV is set finally $E_{LIV} > 1.5 M_{Pl}$.



Constraint on LIV by time lag of different energy photons from GRB 221009A

- **Cross correlation function (CCF).** Light curves of different energy bands are given by the WCDA data. CCF method is adopted to derive the time lags of the different light curves.
- **Maximal likelihood method.** The probability density function (PDF) of a photon at time t and N_{hit} is given. $\lambda(t)$ is the intrinsic light curve with possible time lag $\Delta t_{LIV}(E)$.



$$P(t, N_{hit} | \eta_n, I) \propto \int_0^{\infty} \lambda[t - \Delta t_{LIV}(E, \eta_n)] \gamma(E) \times F(E) A_{N_{hit}}(E) dE; N_{hit} = 0, 1, \dots, 9$$

The stringent LIV constraint by time of flight

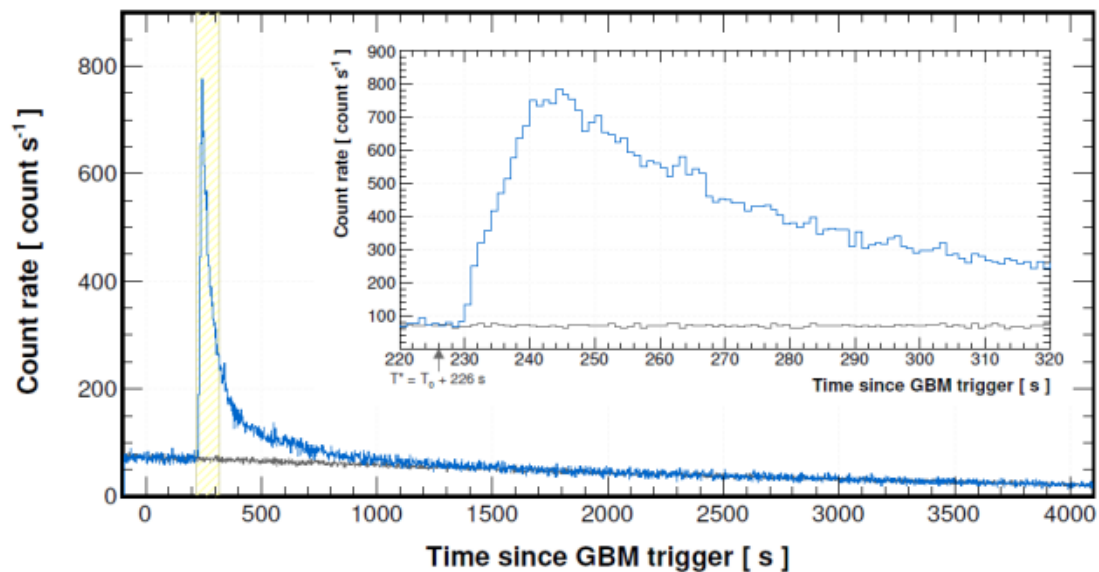
Cao, Z. et al., PRL 2024

- For the 2nd LIV the LHAASO constraint is the best one with 6-8 times improvement to Fermi-LAT result.

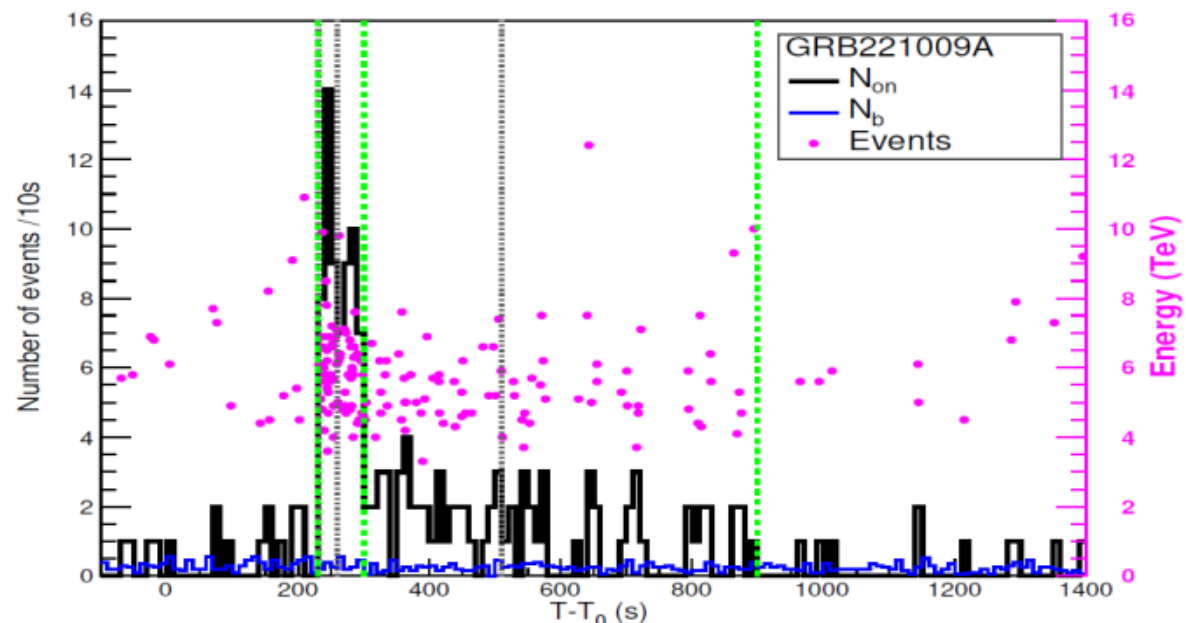
Method	Cross correlation function			Maximum likelihood		
	η^{LL}	η^{BF}	η^{UL}	η^{LL}	η^{BF}	η^{UL}
η_1	-0.25	0.05	0.18	-0.10	0.00	0.10
η_2	-0.60	0.25	0.64	-0.27	0.00	0.29
	superluminal		subluminal	superluminal		subluminal
$E_{\text{QG},1} [10^{20} \text{ GeV}]$	0.5		0.7	1.2		1.2
$E_{\text{QG},2} [10^{11} \text{ GeV}]$	5.0		4.8	7.5		7.2

Combining the KM2A and WCDA data to give a strict limit on LIV

WCDA: 在 3000s 内、 $\sim 0.2-7\text{TeV}$ 范围内探测到了大约 64,000 个光子 (LHAASO Collaboration. Science 380, 1390 (2023))



KM2A: 在 230-900s 内、 $\sim 3-13\text{TeV}$ 范围内探测到了 142 个光子 (LHAASO Collaboration. Science Advances 9 (46) (2023))



利用 KM2A 230-900s 的 142 个光子计算 likelihood function:

$$\mathcal{L} \left(\eta_n \left| \left\{ t^{(i)}, E_{\text{est}}^{(i)} \right\} \right. \right) = \prod_{i=1}^{142} P(t^{(i)}, E_{\text{est}}^{(i)} | \eta_n)$$

Yang, BXJ, Yin, JCAP 04 (2024) 060

定义:

$$L(\eta_n) \equiv -2 \ln \left(\frac{\mathcal{L}_{\eta_n}}{\mathcal{L}_{\hat{\eta}_n}} \right)$$

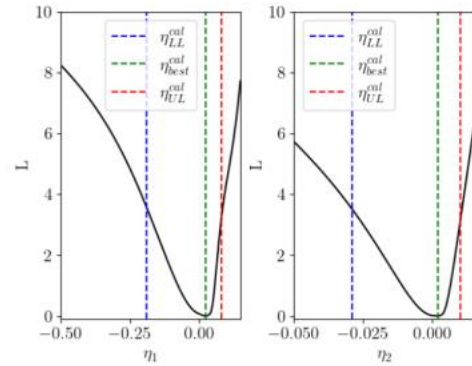


FIG. 3. The $L - \eta_1$ (left) and $L - \eta_2$ (right) curves (black solid lines) of Model-1. The green dashed lines represent the position of $\eta_{\text{best}}^{\text{cal}}$, while the red dashed lines and blue dashed lines indicate the the lower and upper ranges of the 95% CI

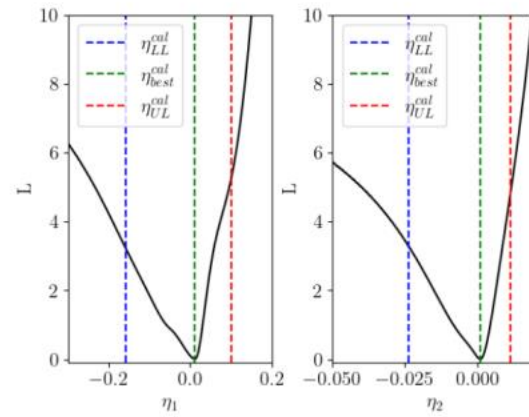


FIG. 4. Same as Fig. 3, but for Model-2.

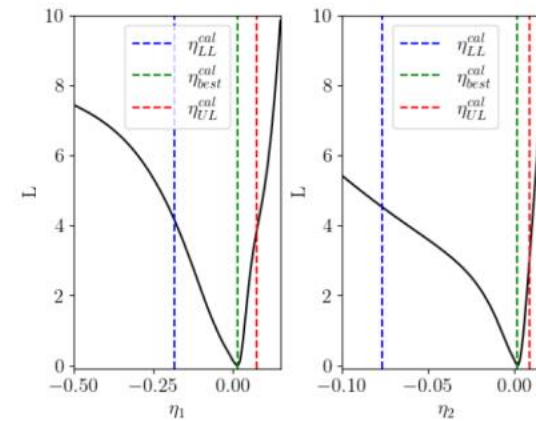


FIG. 5. Same as Fig. 3, but for Model-3.

TABLE II. The calibrated best fits of η_n , the lower and upper bounds of the 95% CIs of η_n , and the corresponding 95% CL lower limits on the E_{QG} .

	$\eta_{\text{LL}}^{\text{cal}}$	η_1^{cal} $\eta_{\text{best}}^{\text{cal}}$	$\eta_{\text{UL}}^{\text{cal}}$	$\eta_{\text{LL}}^{\text{cal}}$	η_2^{cal} $\eta_{\text{best}}^{\text{cal}}$	$\eta_{\text{UL}}^{\text{cal}}$	$E_{\text{QG},1} [10^{19} \text{GeV}]$		$E_{\text{QG},2} [10^{11} \text{GeV}]$	
							$S = +1$	$S = -1$	$S = +1$	$S = -1$
Model-1	-0.189	0.024	0.083	-0.029	0.002	0.010	14.7	6.5	12.0	7.2
Model-2	-0.159	0.011	0.100	-0.024	0.001	0.011	12.2	7.7	11.5	7.9
Model-3	-0.184	0.015	0.074	-0.077	0.002	0.009	16.4	6.6	13.1	4.4

The photons with the maximum energy

- The energy of each photon depend on the true SED, which is SED model dependent.

$$P(E|(E_{rec}, \theta)) = \frac{f(E)A_{eff}(E, \theta)P(E_{rec}|(E, \theta))}{\int f(E)A_{eff}(E, \theta)P(E_{rec}|(E, \theta))dE}$$

$$\xi = \int_0^{E_\xi} P(E|(E_{rec}, \theta))dE$$

$T_{event}(s)$	E_{LP} (TeV)	E_{PLEC} (TeV)	E_{EBL} (TeV)	N_e	N_μ	θ (°)	$\Delta\psi$ (°)	D_{edge} (m)	P (%)
236.6	$12.7^{+6.2}_{-3.8}$	$9.7^{+3.3}_{-2.1}$	$9.8^{+3.1}_{-2.3}$	60.6	0	28.5	0.46	77	7.0
242.5	$10.5^{+5.0}_{-3.2}$	$8.3^{+3.0}_{-2.1}$	$8.4^{+3.2}_{-2.2}$	57.4	0	28.8	0.45	111	10
262.4	$12.6^{+5.5}_{-3.8}$	$9.5^{+3.4}_{-2.3}$	$9.6^{+3.3}_{-2.4}$	57.3	0	28.6	0.53	180	5.7
358.1	$10.0^{+4.8}_{-3.2}$	$7.4^{+3.1}_{-1.8}$	$7.9^{+3.3}_{-2.2}$	46.0	0	28.7	0.54	119	6.0
571.1	$9.4^{+5.1}_{-3.0}$	$7.4^{+2.6}_{-2.5}$	$7.7^{+3.0}_{-2.5}$	45.7	0	29.5	0.52	99	7.8
643.0	$17.8^{+7.4}_{-5.1}$	$12.2^{+3.5}_{-2.4}$	$12.5^{+3.2}_{-2.4}$	81.8	0.3	29.7	0.62	181	4.5
812.4	$11.1^{+5.9}_{-4.3}$	$7.4^{+3.6}_{-2.8}$	$7.6^{+3.9}_{-3.0}$	68.0	0	30.3	0.66	112	11
863.8	$12.9^{+6.1}_{-3.9}$	$9.2^{+3.0}_{-2.8}$	$9.7^{+3.2}_{-3.1}$	100.2	0.8	30.1	1.07	81	17
894.1	$13.6^{+6.1}_{-4.2}$	$9.7^{+3.4}_{-2.5}$	$10.4^{+3.3}_{-3.0}$	60.5	0	31.8	0.83	214	16

TITLE: GCN CIRCULAR

NUMBER: 32677

SUBJECT: LHAASO observed GRB 221009A with more than 5000 VHE photons up to around 18 TeV

DATE: 22/10/11 09:21:54 GMT

FROM: Judith Racusin at GSFC <judith.racusin@nasa.gov>

Summary

- LHAASO has large coverage of muon detector. It has large FOV, wide energy range, high sensitivity and achieves impressive success. Dozens of UHE gamma sources have been observed.
- Complete light curve of GRB 221009A for TeV afterglow was observed by LHAASO. The spectrum was measured from $\sim 200\text{GeV}$ – $\sim 10\text{TeV}$.
- Implications of the measurements on EBL and new physics scenarios are studied. Strong constraints on EBL at large wave length, axion coupling and LIV energy scales are derived.